

SPRINGER BRIEFS IN
APPLIED SCIENCES AND TECHNOLOGY

Hideki Takebayashi

Improvement Measures of Urban Thermal Environment

**SpringerBriefs in Applied Sciences
and Technology**

More information about this series at <http://www.springer.com/series/8884>

Hideki Takebayashi

Improvement Measures of Urban Thermal Environment

Hideki Takebayashi
Graduate School of Engineering
Kobe University
Kobe
Japan

ISSN 2191-530X ISSN 2191-5318 (electronic)
SpringerBriefs in Applied Sciences and Technology
ISBN 978-3-319-13784-1 ISBN 978-3-319-13785-8 (eBook)
DOI 10.1007/978-3-319-13785-8

Library of Congress Control Number: 2014956870

Springer Cham Heidelberg New York Dordrecht London
© The Author(s) 2015

This work is subject to copyright. All rights are reserved by the Publisher, whether the whole or part of the material is concerned, specifically the rights of translation, reprinting, reuse of illustrations, recitation, broadcasting, reproduction on microfilms or in any other physical way, and transmission or information storage and retrieval, electronic adaptation, computer software, or by similar or dissimilar methodology now known or hereafter developed.

The use of general descriptive names, registered names, trademarks, service marks, etc. in this publication does not imply, even in the absence of a specific statement, that such names are exempt from the relevant protective laws and regulations and therefore free for general use.

The publisher, the authors and the editors are safe to assume that the advice and information in this book are believed to be true and accurate at the date of publication. Neither the publisher nor the authors or the editors give a warranty, express or implied, with respect to the material contained herein or for any errors or omissions that may have been made.

Printed on acid-free paper

Springer International Publishing AG Switzerland is part of Springer Science+Business Media
(www.springer.com)

Preface

In Japan, various urban heat island measure strategies have been developed, and their effectiveness has been verified in several applications such as cool roofs, green roofs, cool pavements, heating, ventilating and air conditioning systems with little exhaust heat, and wind paths in urban areas. Based on the various research findings, the Architectural Institute of Japan published the 'Cool Roof Guidebook' in Japanese in March 2014.

The author has lectured to students from the Department of Architecture undertaking the 'urban environmental planning' undergraduate course and to students undertaking the 'urban environment systems' masters course; this book is at a similar level to the content of the lectures. This book provides an overview and a systematic description of the features and effects of urban heat island countermeasure technologies. It also describes the evaluation methods of the countermeasure effects of these technologies. The book is unique because it describes the optimal selection methods of urban heat island countermeasure technologies according to regional climate, topography, land use, urban block form, building shape and location in outdoor spaces, etc.

Most of this book is based on the results of research conducted by the author and Emeritus Professor Masakazu Moriyama, with the cooperation of various collaborative companies, researchers in other universities and research institutes, and many students from Kobe University. This book is a cooperative achievement between Emeritus Professor Masakazu Moriyama and the author. We received valuable advice regarding cool roof and cool pavement research from Prof. Hashem Akbari of Concordia University, Canada, who is a leading expert in this field. We also received various advice and ideas about climate analysis for urban planning from Prof. W. Kuttler, Prof. H. Mayer, Prof. J. BaumueUler, Prof. E. Parlow, Prof. G. Gross, and Prof. A. Matzarakis of Germany. The author is very grateful to everyone for the support he received from Japan and overseas.

Contents

1	Improvement Measures of Urban Thermal Environment	1
1.1	Outline of Urban Heat Island Measure Strategies	1
1.1.1	An Urban Heat Budget Model and Air Temperature Near the Ground Surface	3
1.1.2	Effect of the Heat Budget on Urban and Natural Areas	4
1.2	Improving Surface Cover	5
1.2.1	Places Where the Surface Temperature Tends to Rise	5
1.2.2	Street Canyon Characteristics and Solar Radiation Gains.	10
1.2.3	Effects of Urban Heat Island Measure Techniques on Surface Cover.	12
1.2.4	Appropriate Selection of Urban Heat Island Measure Techniques.	23
1.3	Reduction of Exhaust Heat	28
1.3.1	Reduction of Cooling Load.	29
1.3.2	Improving the Heat Release Method	29
1.4	Improving Ventilation.	31
1.4.1	Wind as a Climate Resource	31
1.4.2	Ventilation in Street Canyons	36
1.5	Conclusions.	39
	References.	41

Author Biography

Hideki Takebayashi is an Associate Professor of the Department of Architecture, Graduate School of Engineering, Kobe University. He obtained his Doctorate in Engineering from Kobe University, under the supervision of Prof. Masakazu Moriyama. He took over the Urban Environmental Engineering Laboratory at the Department of Architecture from Emeritus Professor Masakazu Moriyama. His research focuses on the optimal selection method of urban heat island countermeasure technologies according to regional climate, topography, land use, urban block form, building shape and location in outdoor spaces, etc. He is an active member of the Osaka Heat Island Countermeasure Technology Consortium, and the Heat Island Institute International and Architectural Institute of Japan. He is chair of the Cool Roof Appropriate Dissemination Subcommittee at the Architectural Institute of Japan, which published the 'Cool Roof Guidebook'.

Chapter 1

Improvement Measures of Urban Thermal Environment

Abstract Specific measures for the urban heat island phenomenon are summarized in the following three points; improving surface cover, reducing exhaust heat, and improving ventilation. With regard to improving surface cover, the appropriate heat island measure techniques on surface cover, i.e., cool roofs, green roofs, and cool pavements, etc., should be preferentially introduced in places where the surface temperatures tend to rise. The effects of urban heat island measure techniques on surface cover are evaluated by surface heat budget on each surface and by solar radiation shielding effects by street trees. With regard to reducing exhaust heat, measures for reducing exhaust heat released from the outdoor units of air conditioners are the reduction of cooling loads in rooms and improving heat release methods. Various energy saving strategies have been proposed. Improving the release method of anthropogenic heat so as not to contribute to rises in the air temperature is one of the heat island measures. With regard to improving ventilation, preventing heat from staying in the street canyons by improving ventilation near the ground surface is one of the heat island measures. Suppressing the building coverage ratio leads to improvements in ventilation in street canyons. Ventilation in street canyons is improved on wider roads parallel to the main wind direction.

1.1 Outline of Urban Heat Island Measure Strategies

The urban heat island phenomenon, i.e., increased air temperature in urban areas, is recognized as a serious problem in Japan. Various urban heat island measure strategies have been developed, and their effectiveness has been verified in several applications, such as cool roofs, green roofs, cool pavements, heating, ventilation and air conditioning systems with little exhaust heat, and wind paths in urban areas. Specific measures for the urban heat island phenomenon are summarized under the following three points:

- Improving surface cover
- Reducing exhaust heat
- Improving ventilation

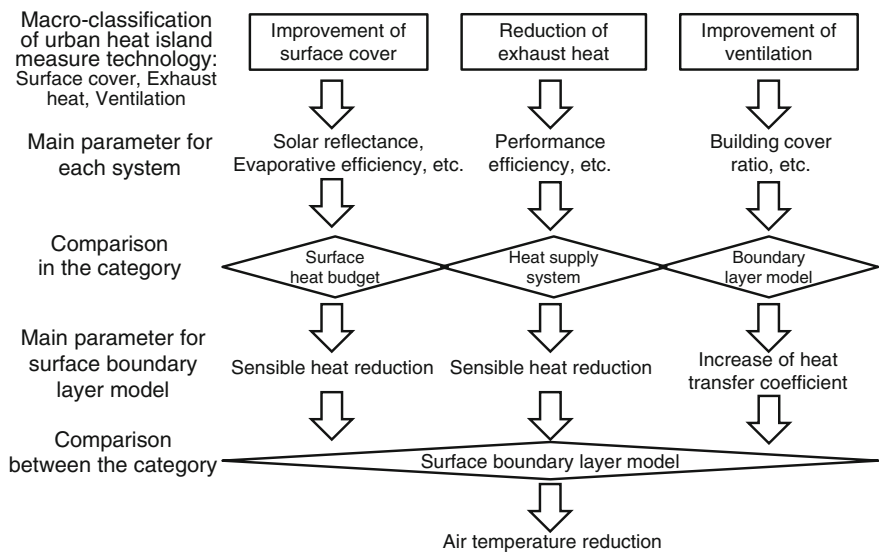


Fig. 1.1 General evaluation process of urban heat island measure effects

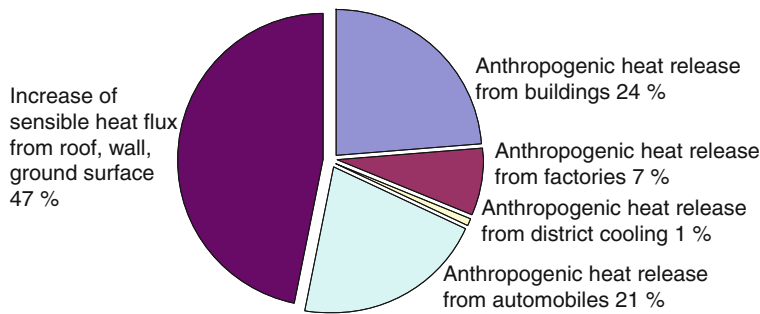


Fig. 1.2 Increased ratio of sensible heat flux (daily average in 23 wards of Tokyo)

The general evaluation process of the urban heat island measure effect is shown in Fig. 1.1 [1]. The heat island measure effects are obtained (a) by reducing sensible heat flux from the surface cover by suppressing surface temperature rise as a heat source, (b) by suppressing exhaust heat released from automobiles and air conditioner outdoor units, and (c) by increasing heat transfer from the surface to the upper air by dissipating the heat by better ventilation. The increased ratio of the daily average of sensible heat flux in 23 wards of Tokyo is shown in Fig. 1.2 [2]; almost half of the increase of sensible heat flux is from the surface cover and the other half is from anthropogenic heat release. Therefore, urban heat island countermeasures should be carried out in a well-balanced manner.

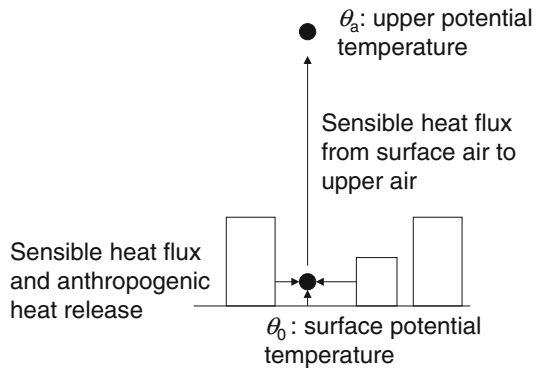
1.1.1 An Urban Heat Budget Model and Air Temperature Near the Ground Surface

The air temperature near the ground surface becomes high due to positive sensible heat flux from the surface to the air and becomes low due to negative sensible heat flux from the surface to the air. In other words, the air temperature rises when the surface temperature is higher than the air temperature and falls when the surface temperature is lower than the air temperature. However, even if the same sensible heat flux comes from the surface to the air, the rise in air temperature is not the same at any given time.

Heat budget near the ground surface indicating the status of surface air temperature is represented by the surface boundary layer model which is shown in Fig. 1.3 [3]. Both sensible heat flux from the surface to the air and anthropogenic heat from outdoor air conditioner units and automobiles are released into the air near the ground surface. Not all of these heat fluxes cause the air temperature to rise near the ground surface. Most of these heat fluxes are transferred into the upper air from near ground surface air; however, some of these heat fluxes cause the air temperature to rise near the ground surface.

In the surface boundary layer model, if the sensible heat flux or anthropogenic heat released into the air near the ground surface is small or the sensible heat flux transported from the air near the ground surface to the upper air is large, the air temperature near the ground surface falls. When the wind velocity of the upper air is high and the temperature difference between the upper air and near ground surface air is large during the day time, the comprehensive convective heat transfer coefficient from near ground surface air to the upper air is large. As a result, since sensible heat flux transported from the near ground surface air to the upper air is large, the air temperature near the ground surface does not increase very much, even if the sensible heat flux from the surface to the air is large. At night time, since the wind velocity of the upper air is low and the temperature difference between the upper air and near ground surface air is small, the comprehensive convective heat transfer coefficient from the near ground surface air to the upper air is small. As a result, since sensible heat flux transported from the near ground surface air to the upper air is small,

Fig. 1.3 Surface boundary layer model



upper air is small, the rise in the air temperature near the ground surface is relatively large, even if the sensible heat flux from the surface to the air is small.

Air temperature near the ground surface is evaluated by a three-dimensional mesoscale numerical weather simulation model such as the MM5 or WRF (University Corporation for Atmospheric Research) because air temperature is also affected by geographical features, i.e., close to the sea or mountains, or an urban or suburban location, etc. This model is very simple if the upper weather conditions are accurately provided and the air temperature near the ground surface is generally reproduced.

1.1.2 Effect of the Heat Budget on Urban and Natural Areas

The effect of the heat budget on urban and natural areas is shown in Fig. 1.4 [2]. Solar radiation and the reflectance of solar radiation are almost the same on urban and natural areas. Solar reflectance from trees is not large. Solar reflectance on urban areas is not large due to the shadows from buildings and dark-colored asphalt in spite of light-colored concrete. As a result, the difference in solar radiation between urban and natural areas is small. Therefore, it is thought that the benefits of applying high-reflectance paint to urban areas are relatively high. A slightly larger amount of radiation from the sky is found in urban areas due to air pollutants and a slightly larger amount of radiation from the ground surface is also found in urban areas due to the high surface temperatures, making only a small difference in net radiation between urban and natural areas.

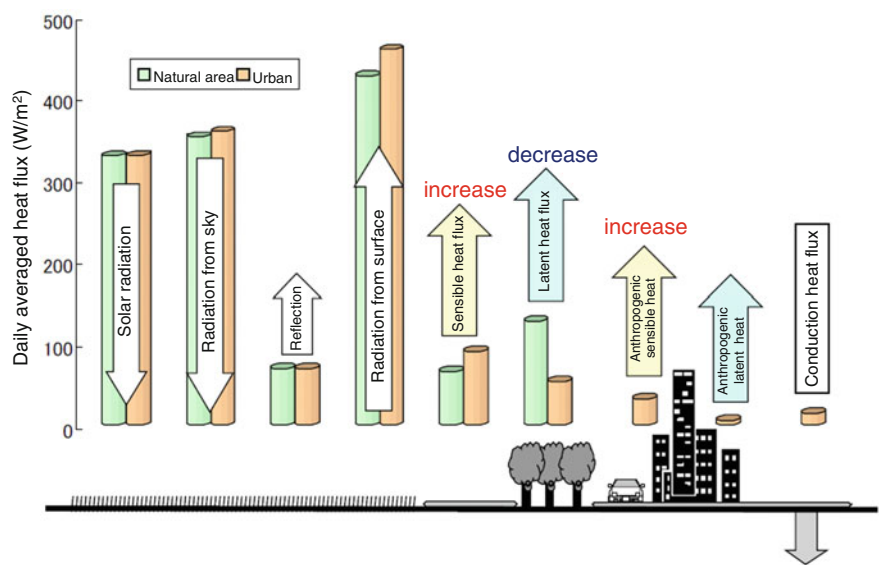


Fig. 1.4 Effects of heat budget on urban and natural areas

Sensible heat flux from urban areas is larger than from natural areas, since latent heat flux from urban areas is smaller than natural areas due to the small amount of natural land cover, such as greenery, soil and surface water. Large amounts of anthropogenic sensible and latent heat from air conditioning units or automobiles are found in urban areas, which contribute to rises in air temperature and humidity. However, since latent heat flux from urban areas is small, the rise in humidity from anthropogenic latent heat is not so remarkable.

1.2 Improving Surface Cover

Appropriate heat island measure techniques on surface cover, i.e., cool roofs, green roofs, cool pavements, etc., should preferentially be introduced at the places where the surface temperature tends to rise, and the most effective techniques should be selected for the target place; these should be determined by predicting the effect of each technique, as far as possible.

1.2.1 Places Where the Surface Temperature Tends to Rise [4]

The air temperature in outdoor spaces tends to rise when the surrounding surface temperature is high. The surface temperature is increased mainly by solar radiation and decreased by radiative cooling. Examples of calculation results of surface temperature distribution on the street of an urban area are shown in Fig. 1.5; it is reflected

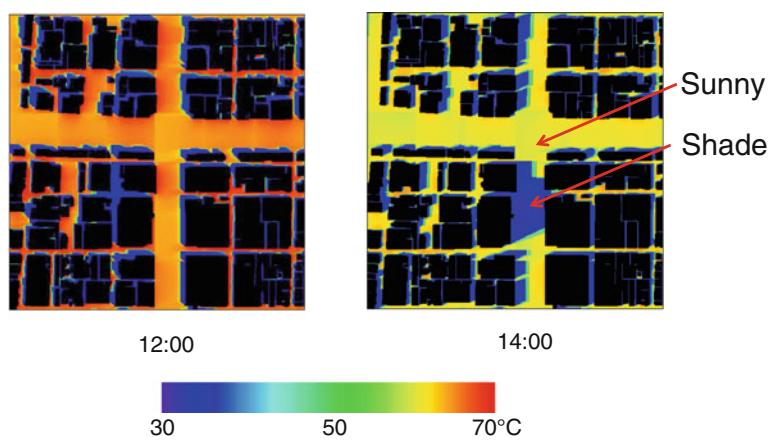
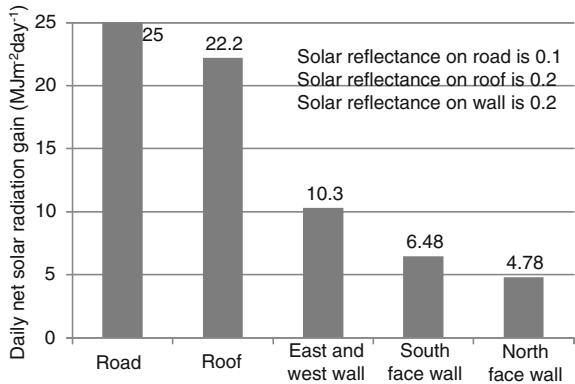


Fig. 1.5 Examples of surface temperature distribution on the street at 12:00 and 14:00 on a typical fine summer day

Fig. 1.6 Daily net solar radiation gains in summer on each surface of an isolated building



by the distribution of solar radiation. The surface temperature is high in sunny places and low in shady places. It has been calculated by taking into account the history of the solar radiation received at each point; however, its effect is not clear. Therefore, heat island measure techniques are required at the places where the surface temperatures are higher throughout the day due to the larger daily integration solar radiation.

1.2.1.1 Isolated Buildings

Daily net solar radiation gains in summer on each surface of an isolated building are shown in Fig. 1.6. The calculations are based on an approximate latitude of 35°N (assumed to be in the central Osaka area) and similar conditions apply to the following. The reason that the gain on the road is greater than on the roof is the lower solar reflectance. Daily net solar radiation on the road and roof is higher than on the wall because of the greater solar altitude. Daily net solar radiation on the east and west surfaces is larger than on the north and south surfaces of the wall. Therefore, the roof and road surfaces have a higher priority as heat island mitigation locations under general summer conditions in mid-latitude regions.

1.2.1.2 A Simple Urban Canyon Model

The daily net solar radiation gain on an east–west road is shown in Fig. 1.8. A simple urban canyon model that considers only the aspect ratio (W/H) is shown in Fig. 1.7. Road width (W) and building height (H) are varied as a reference aspect ratio (W/H) of 1 ($W = H = 15$ m). The distribution is dominated by the shadows of the buildings to the south. High-priority areas for urban heat island mitigation measures extend to the buildings on the south side of the roads for street canyons with larger W/H ratios.

Daily net solar radiation gains on north–south roads are shown in Fig. 1.8. The distribution is dominated by the shadows of the buildings on both sides of the road. Other priority locations for urban heat island mitigation measures are the areas around the center of the roads for models with larger W/H ratios.

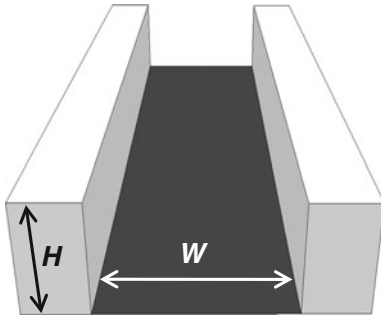


Fig. 1.7 A simple urban canyon model that considers only the aspect ratio (W/H)

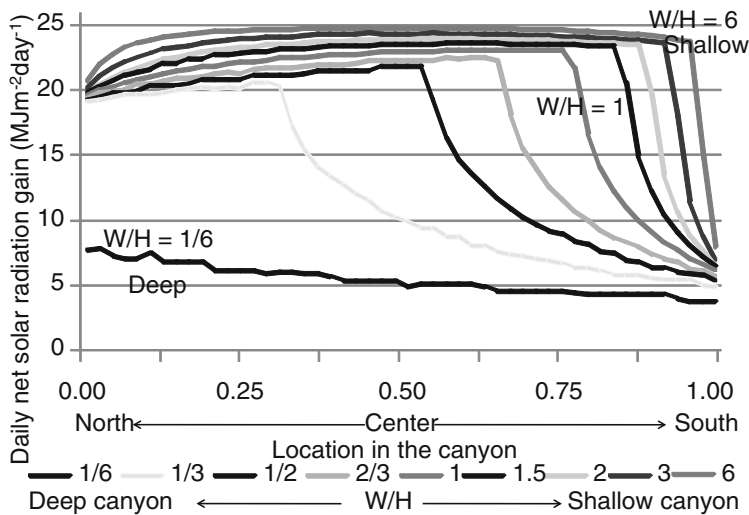


Fig. 1.8 Daily net solar radiation gains for various aspect ratios on an east–west road

Daily net solar radiation gains at intersections are an integrated distribution of those shown in Figs. 1.8 and 1.9. The amounts of daily net solar radiation gain in the areas close to the north sides are large, as shown in Fig. 1.8. Furthermore, those in the southern areas are large around the centers of the roads owing to the influence of the shadows of southwest and southeast buildings, as shown in Fig. 1.9.

1.2.1.3 Building Models with Non-uniform Building Heights

Daily net solar radiation gains on roofs affected by taller adjacent buildings are shown in Figs. 1.11 and 1.12. A building model that incorporates the height difference (ΔH) and the distance (D) from the tallest building is shown in Fig. 1.10. It

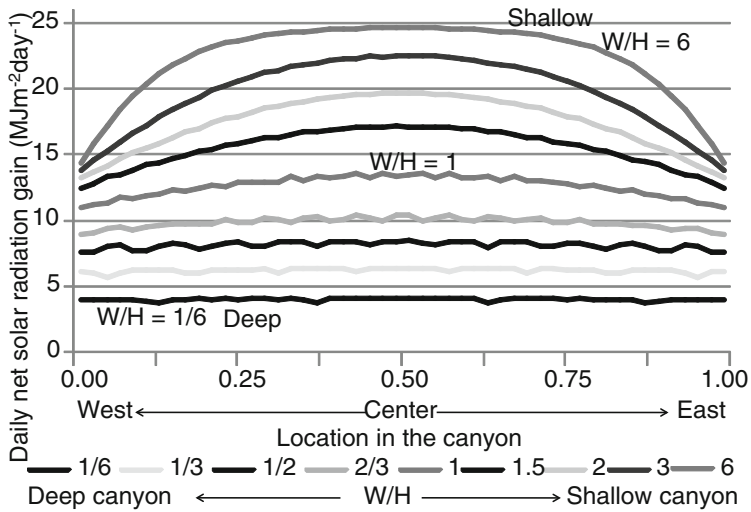
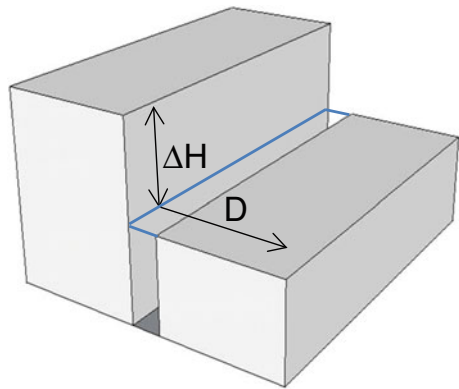


Fig. 1.9 Daily net solar radiation gains for various aspect ratios on a north–south road

Fig. 1.10 Buildings model incorporating the height difference (ΔH) and the distance (D) from the tallest building



is assumed that a 15, 30, or 60 m taller building is located at the center of the figure and the target roof is away from the tallest building with the horizontal axis in the north–south direction in Fig. 1.10 and the west–east direction in Fig. 1.12.

The daily net solar radiation gain on the roof of a building located on the north side of a taller building is greatly reduced in the vicinity of the taller building, but the affected area is relatively small. The radiation gain on the roof of a building on the west or east side of a taller building is generally reduced at short distances from the taller building, and the affected area is somewhat larger. The low solar altitudes in the morning and evening periods affect the daily solar gains on adjacent shaded

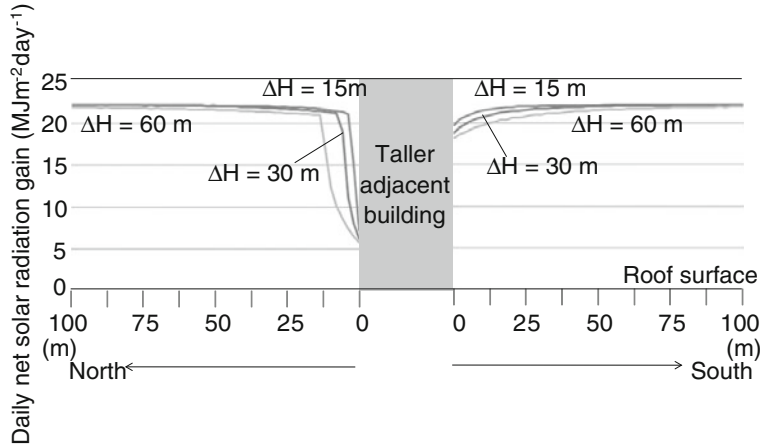


Fig. 1.11 Effects of a taller building adjacent to the north or south side of the target building on solar radiation gains

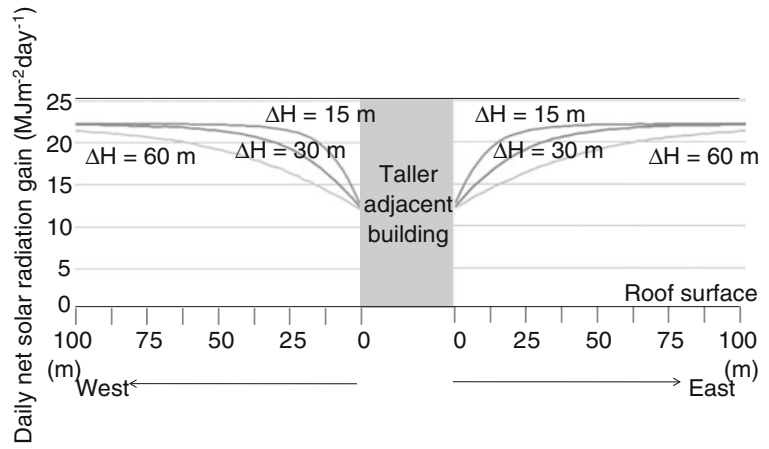


Fig. 1.12 Effects of a taller building adjacent to the north or south side of the target building on solar radiation gains

buildings. Even if a 60 m taller building is located on the south side of the target building, the shadow effect caused by the taller building is small when the distance between the buildings is more than 15 m. If the target building is located on the west or east side of the taller building, the affected area varies depending on the differences in height between the buildings. In addition, if the target building is located to the northwest or northeast of a taller building, the affected area is formed by combining Figs. 1.11 and 1.12.

1.2.2 Street Canyon Characteristics and Solar Radiation Gains [4]

The distribution of daily net solar radiation gains on the roofs in the central business district of Osaka city is shown in Fig. 1.13. We analyzed the relationship between street canyon characteristics and solar radiation gains. A comparison of the proportions represented by each horizontal surface type within an aerial view with the proportions of daily net solar radiation gains for each of those surfaces and for walls in the central Osaka area is shown in Fig. 1.14. The daily net solar radiation gains for roads are less than those in the areas they represent because of the radiation gains for wall surfaces. In particular, the 23:14 ratio of the aerial view to the solar radiation gain for north–south roads is attributed to the large radiation gains on east and west walls. The daily net solar radiation gains on the roofs are not decreased on the buildings along wide roads, because they are not affected by the shade of the surrounding buildings. Furthermore, the radiation gains for the other buildings are not decreased, because the effects of the shade and the reflections from the surrounding buildings offset each other. The relationships between the components of an urban street canyon and their daily net solar radiation gains are shown in Fig. 1.15. The daily net solar radiation gains are largest on roof surfaces, followed by east–west roads, north–south roads, and walls. In the roof category, radiation gains are less on smaller buildings with low heights that are shaded by surrounding buildings. In the road category, radiation gains on east–west roads are larger than those on north–south roads because the shadows on east–west roads from surrounding buildings are less than those on north–south roads in the summer. The large standard deviations are due to large variations in the sunlight and shade on the

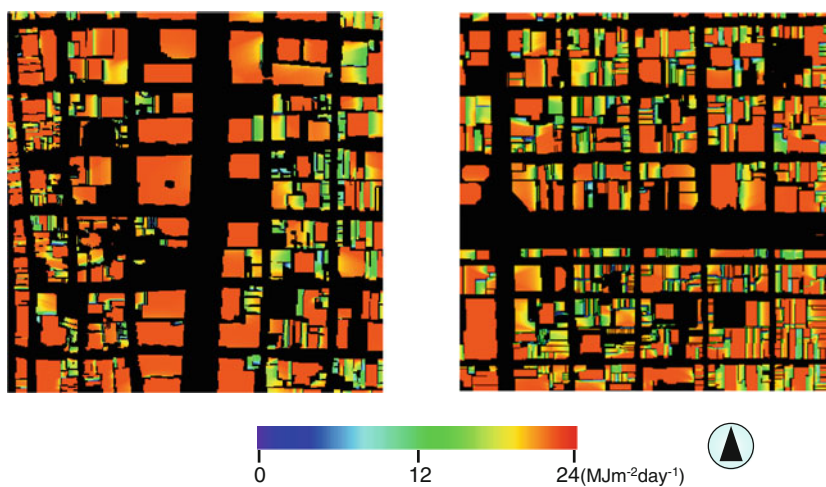


Fig. 1.13 Distribution of daily net solar radiation gains on the roofs in the central business district of Osaka city

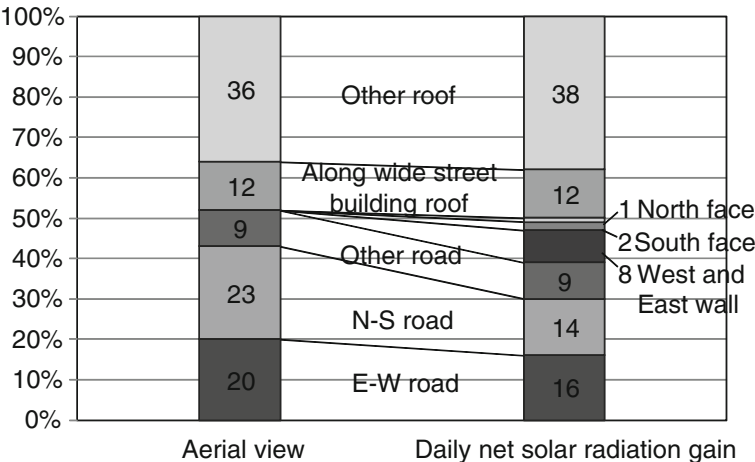


Fig. 1.14 Proportion of aerial views and daily net solar radiation gains for various surfaces in the central Osaka area

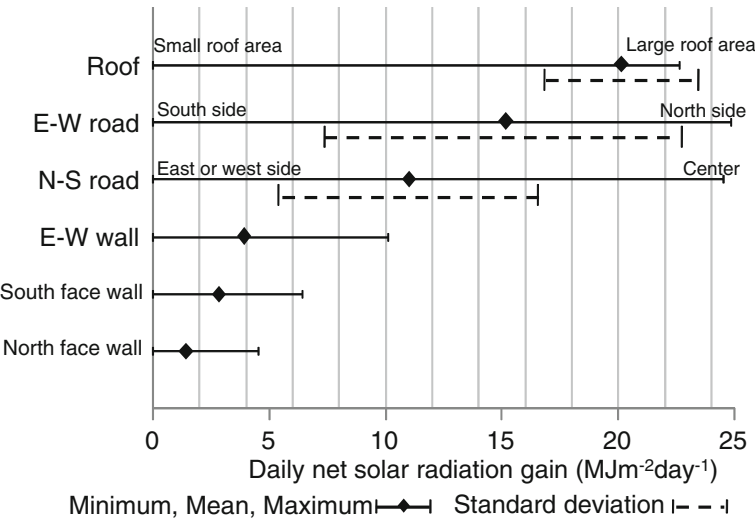


Fig. 1.15 Components of an urban street canyon and their daily net solar radiation gain levels and variations

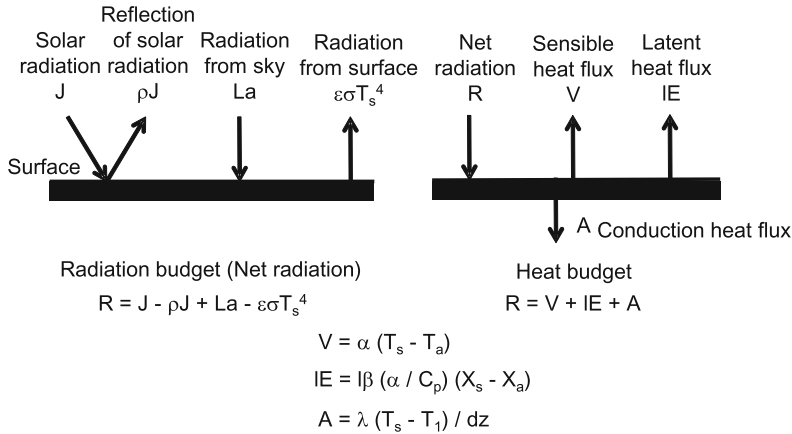
north and south sides of east–west roads. In the wall category, the solar gains on west and east walls are larger than those on north and south walls owing to the solar altitude in the summer.

1.2.3 Effects of Urban Heat Island Measure Techniques on Surface Cover

1.2.3.1 Surface Heat Budget and Surface Temperature

Diurnal surface temperature change is explained by surface heat budget. Surface temperature rises by solar radiation and declines by radiative cooling. Surface heat budget model components are shown in Fig. 1.16 [5]. The radiation budget is shown on the left side and the heat budget is shown on the right side. The arrows that flow to and from the surface indicate heat flux; these fluxes are balanced on certain surface temperatures. Therefore, surface temperature is obtained by solving the surface heat budget equation.

These heat fluxes occur at the same time. For convenience, the radiation balance is explained first. Net radiation (R) is composed of solar radiation (J), reflection of solar radiation (ρJ), radiation from the sky (La) and ground surface ($\varepsilon\sigma T_s^4$). Solar radiation (J) is given as weather conditions. Reflection of solar radiation (ρJ) is calculated by multiplying the solar reflectance (ρ) of surface to solar radiation (J). Solar reflectance (ρ) is large on light-colored surfaces and small on dark-colored surfaces. Radiation from the sky (La) which is given as weather conditions is small in a clear sky with less water vapor and large in a sky that is covered by water vapor or obstacles such as buildings and plants. Radiation from the ground surface ($\varepsilon\sigma T_s^4$) is large at high surface temperatures (T_s).



Here, R is net radiation (W/m^2), V is sensible heat flux (W/m^2), IE is latent heat flux (W/m^2), A is conduction heat flux (W/m^2), ρ is solar reflectance (-), J is solar radiation (W/m^2), La is radiation from sky (W/m^2), ε is emmissivity (-), σ is Stefan-Boltzmann coefficient ($= 5.67 \times 10^{-8} W/(m^2 K^4)$), T_s is surface temperature (K), T_a is air temperature (K), α is convective heat transfer coefficient ($W/(m^2 K)$), l is latent heat ($= 2512$ kJ/kg), β is evaporative efficiency (-), C_p is specific heat of air ($= 1.0$ kJ/(kgK)), X_s is saturated humidity (kg/kg), X_a is air absolute humidity (kg/kg), λ is thermal conductivity ($W/(mK)$), T_1 is internal temperature (K) of the solid in Δz (m) inside.

Fig. 1.16 Surface heat budget model and heat budget components

Net radiation (R) is combined with sensible heat flux (V), latent heat flux (IE) and conduction heat flux (A), as surface heat balance. Net radiation (R) is positive during the day due to the large amount of solar radiation (J) and negative (called radiative cooling) during the night due to the large amount of radiation from the surface ($\varepsilon\sigma T_s^4$).

Sensible heat flux (V) is transferred from the surface (T_s) to the air (T_a) by the wind. Convective heat transfer coefficient (α) is large during high wind velocity and large temperature differences ($T_s - T_a$).

Latent heat flux (IE) is taken away by evaporation (E) of surface water, which is high at large evaporative efficiency (β), large humidity difference ($X_s - X_a$), and large convective transfer coefficient (α/C_p). Evaporative efficiency (β) is dependent on surface wetness, and is high on evaporative surfaces that contain much water.

Conduction heat flux (A) is transferred by thermal conduction from the surface (T_s) to the inside (T_1) of a solid (Δz), and is high during large heat conductivity (λ) and large temperature differences ($T_s - T_1$).

1.2.3.2 Countermeasures for Surface Temperature Rises

If net radiation (R) is large, the surface temperature is high due to large heat generation on the surface. If sensible heat flux (V), latent heat flux (IE) and conduction heat flux (A) are large, the surface temperature is low due to large heat transfer into the air or inside of a solid. However, if sensible heat flux (V) is large, air temperature may become high due to the heat transferred from the surface to the air. Moreover, if conduction heat flux (A) is large, indoor air temperatures may become high due to heat conducted through the wall or roof. Therefore, to reduce net radiation (R) and to increase latent heat flux (IE) are more appropriate urban heat island measures.

To reduce net radiation (R), it is necessary to increase solar reflectance (ρ) and emissivity (ε) of the surface, and to reduce solar radiation (J) and radiation from the sky (La). Specific measures are high-reflectance coatings and materials, and shielding solar radiation by street trees or awnings, etc.

To increase latent heat flux (IE), it is necessary to increase evaporative efficiency (β) and the transfer coefficient of water vapor (α/C_p). Specific measures are green roofs, walls and pavements, water-retentive materials, surface water, and improvement of ventilation in street canyons, etc.

From the above-mentioned facts, the main parameters are solar reflectance (ρ) and evaporative efficiency (β). As heat island countermeasures on roof surfaces has the highest priority, the calculated average results of sensible heat flux and surface temperature of various heat island techniques such as cool roofs and green roofs at 13:00 in summer (from 18 July to 15 September, 2005 at Osaka Japan) are shown in Fig. 1.17 [1]. Increases of surface temperature and sensible heat flux which cause heat island are prevented by evaporative cooling and solar reflection. Evaporative cooling occurs on green roofs, water retention materials, green walls, surface sprinklers, and surface water (roof ponds, fountains), etc. Larger solar reflection occurs on cool roofs (paint, sheets, tiles), cool walls, and cool pavements, etc. Greater reductions of the effects of sensible heat flux and surface temperature are seen in cases of large evaporative efficiency or

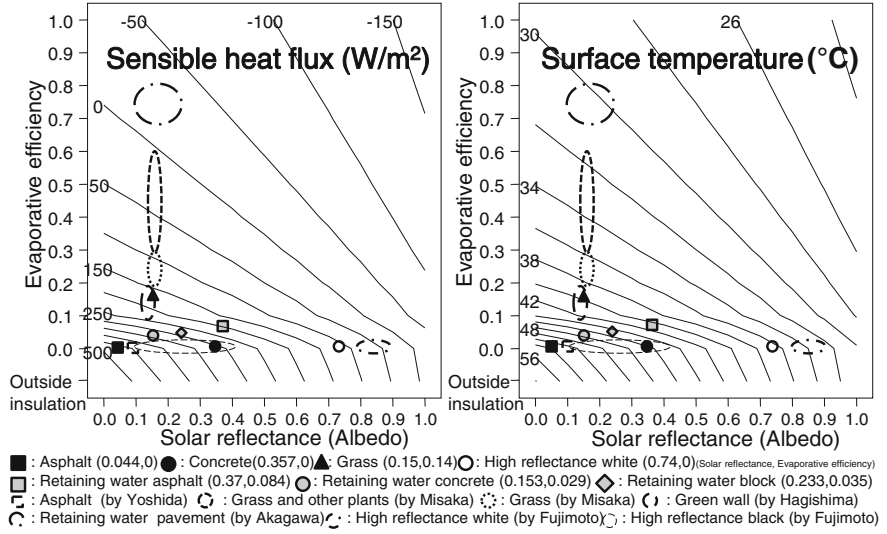


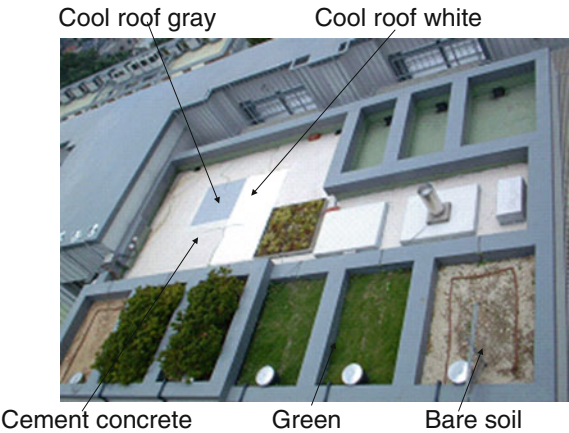
Fig. 1.17 Calculated average results of sensible heat flux and surface temperature at 13:00 in summer (from 18 July to 15 September, 2005 at Osaka, Japan)

large solar reflectance. Evaporation efficiency is represented on the vertical axis and solar reflectance is represented on the horizontal axis in Fig. 1.17. Asphalt and concrete surfaces are plotted on the lower left side. Evaporative (green) roofs are plotted on the upper side and cool roofs are plotted on the right side. The heat island measure effect is greater if the evaporative efficiency or solar reflectance is larger.

1.2.3.3 Surface Heat Budget on Various Surfaces [5, 6]

Surface heat budget experiments on roofs and pavements are shown in Figs. 1.18 and 1.19. Net radiation (R) is observed on each surface by a net radiation meter with

Fig. 1.18 Surface heat budget experiments on a roof



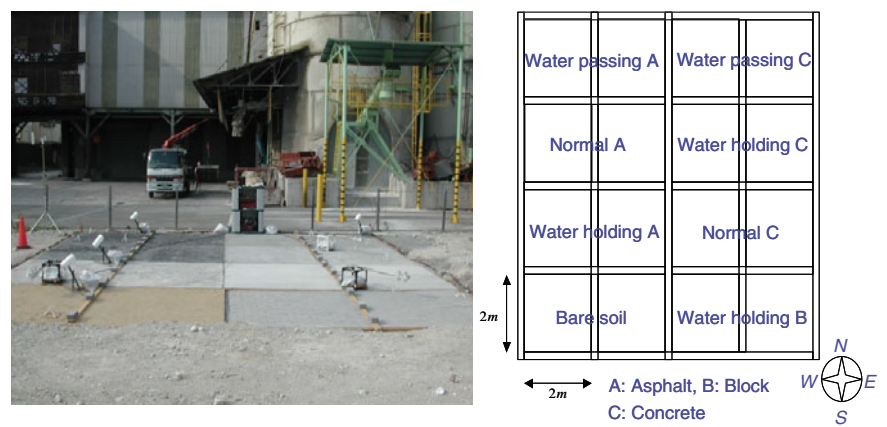


Fig. 1.19 Surface heat budget experiments on a pavement

4 sensors for solar radiation (J), reflection of solar radiation (ρJ), radiation from sky (La) and from the ground surface ($\epsilon\sigma T_s^4$). By analyzing net radiation, the solar reflectance on each surface is obtained using the observed data. Evaporation flux (E) and latent heat flux (IE) are estimated using the observed data of water content ratio in the soil or weight of the materials including the water content. Conduction heat flux (A) is estimated using the observed data of the inner temperature profile or heat flux in a solid. Sensible heat flux (V) is estimated by the eddy correlation method or gradient method. However, since these methods require a large target surface area, sensible heat flux (V) is often calculated by the residual of the heat budget equation.

Surface heat budgets on asphalt, concrete, green roofs, white high-reflectance paint (cool roof white), gray high-reflectance paint (cool roof white), water-retentive asphalt, water-retentive concrete, and water-retentive blocks are shown in Figs. 1.20, 1.21, 1.22, 1.23, 1.24, 1.25, 1.26 and 1.27. The characteristics of surface heat budget on each surface are as follows.

On asphalt surfaces, the net radiation is large due to small solar reflectance, and sensible heat flux is large due to no evaporation. Large sensible heat flux contributes to urban heat island.

On concrete surfaces, the net radiation is smaller than on asphalt due to a slightly larger solar reflectance; however, sensible heat flux is relatively large due to no evaporation.

On green roofs, the net radiation is large due to small solar reflectance; however, sensible heat flux is small due to large evaporation. Small sensible heat flux contributes to urban heat island mitigation.

On white high-reflectance paint, the net radiation is very small due to large solar reflectance; therefore, sensible heat flux is small in spite of no evaporation. Small sensible heat flux contributes to urban heat island mitigation.

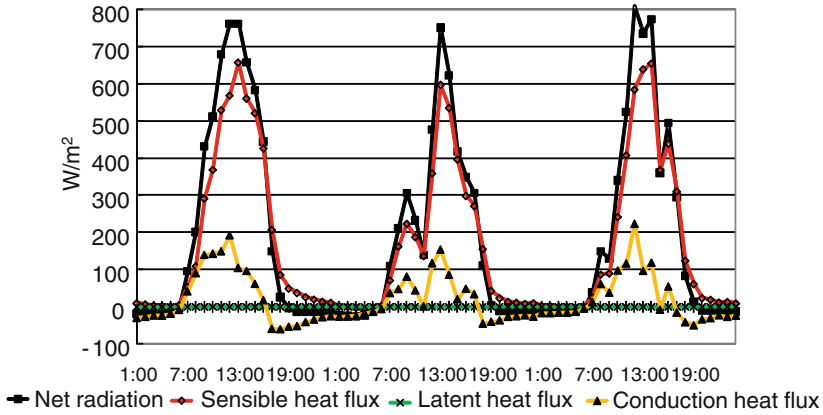


Fig. 1.20 Surface heat budget components on asphalt, August 9–12, 2005

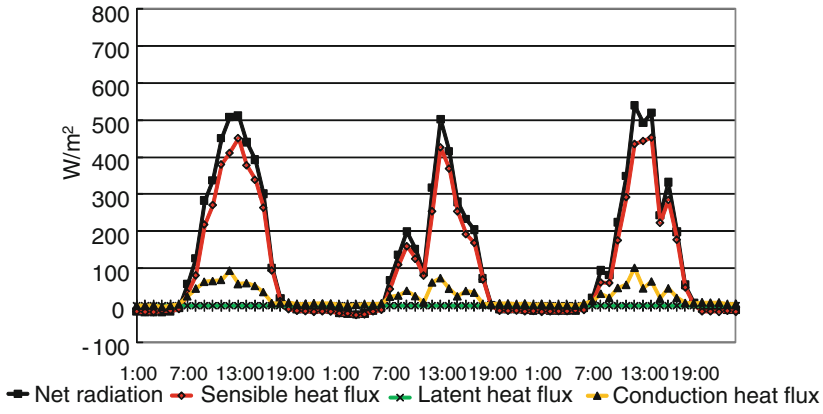


Fig. 1.21 Surface heat budget components on concrete, August 9–12, 2005

On gray high-reflectance paint, the net radiation is not so large due to slightly larger solar reflectance, and sensible heat flux is almost the same as light-colored concrete in spite of no evaporation.

On water-retentive asphalt, the net radiation is not so large due to the white water-retentive material inserted between the aggregates; therefore, sensible heat flux is not so large because it is also affected by evaporation.

On water-retentive concrete, the net radiation is large due to small solar reflectance influenced by the shadow between aggregates; therefore, sensible heat flux is large in spite of evaporation.

On water-retentive blocks, the net radiation is slightly smaller due to the light color; however, sensible heat flux is not small due to little evaporation.

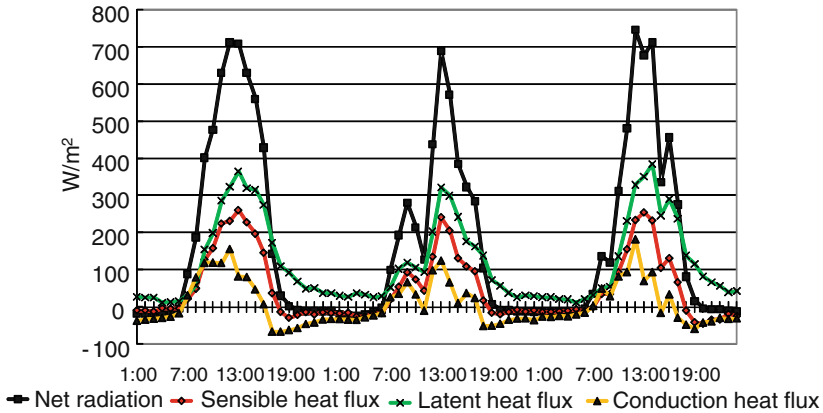


Fig. 1.22 Surface heat budget components on green roofs, August 9–12, 2005

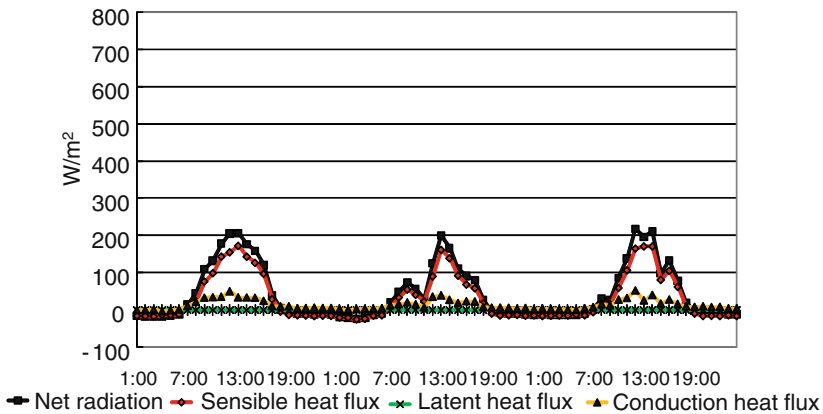


Fig. 1.23 Surface heat budget components on white high-reflectance paint, August 9–12, 2005

Surface temperature and sensible heat flux on various surfaces are shown in Figs. 1.28 and 1.29. Since surface temperature, which is the temperature balance of each heat budget component, reflects the characteristics of heat budget on each surface, sensible heat flux, which is the cause of urban heat islands, depends mainly on surface temperature.

1.2.3.4 Surface Temperatures on Grass Parking Lots and Japanese Tile Roofs [7, 8]

Surface heat budget experiments on parking lots and thermal images are shown in Fig. 1.30. These are observation results at 12:00 and 21:00 on a typical fine summer day. There are thirty-six parking lots built by different private companies, and each

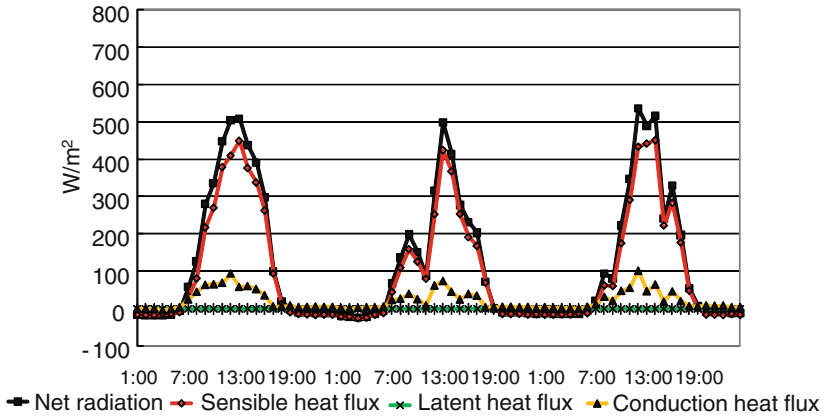


Fig. 1.24 Surface heat budget components on gray high-reflectance paint, August 9–12, 2005

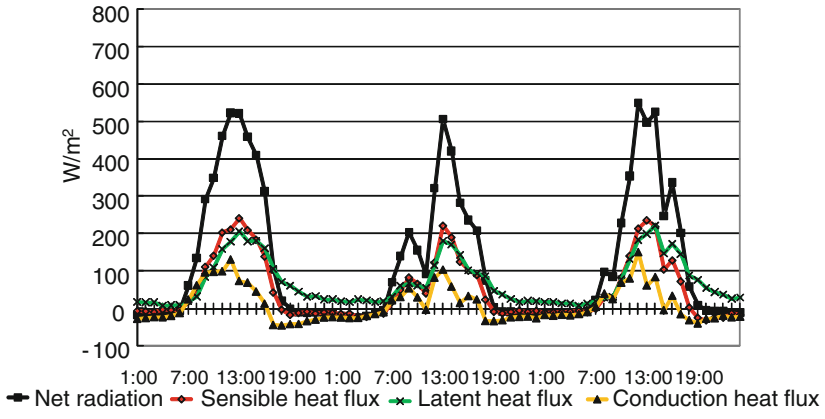


Fig. 1.25 Surface heat budget components on water-retentive asphalt, August 9–12, 2005

parking lot is maintained by each company. Observation results of surface temperatures on each parking lot are shown in Fig. 1.31. The surface temperature is lower on grass and higher on concrete and wood which are in place to bear the weight of the car. The surface temperature on the protector-type parking lot which bears a uniformly distributed load is relatively low due to the large grass-covered area. However, measurements of engine heat and car load are also important.

Surface heat budget experiments on tile roofs and thermal images are shown in Fig. 1.32. These are observation results at approximately 15:00 on a typical fine summer day. The relationship between luminosity and solar reflectance of traditional Japanese roof tiles is shown in Fig. 1.33. Solar reflectance on the tile surface depends on the surface color. The surface temperature on light-colored tiles is low due to large solar reflectance. The view factors of each surface of typical Japanese roof tiles

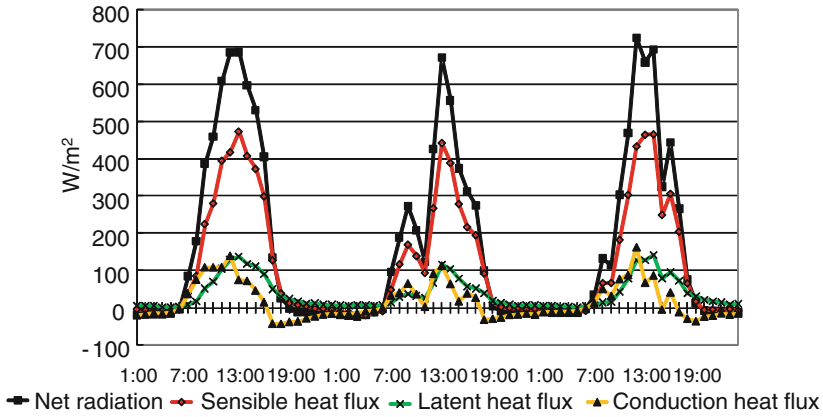


Fig. 1.26 Surface heat budget components on water-retentive concrete, August 9–12, 2005

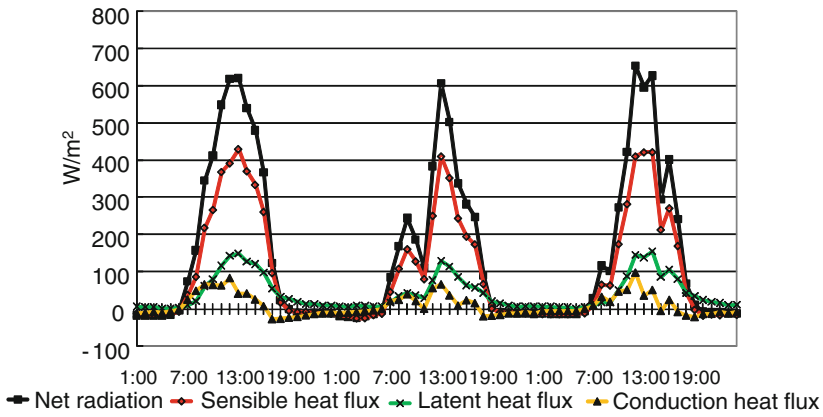


Fig. 1.27 Surface heat budget components on water-retentive block on August 9–12, 2005

are shown in Fig. 1.34. The types of tile are J, S, F, and the decrease of solar reflectance due to the inter-reflection between the surfaces is only a few percent.

1.2.3.5 Summary of the Effect of Urban Heat Island Measure Technologies on Surface Heat Budget

Several research papers have evaluated various kinds of heat island measure technologies previous studies. A summary of the effects of heat island measure technology for the appropriate use of cool roofs has been prepared by a working group for the Architectural Institute of Japan (Table 1.1) [1, 9]. As all the technologies are developed for the purpose of heat island measure, the heat island measure effect of

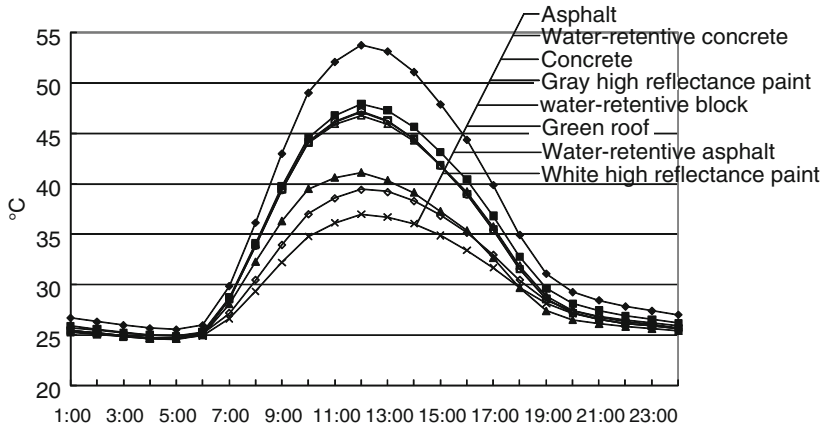


Fig. 1.28 Average surface temperature on various surfaces during the summer period of 2005

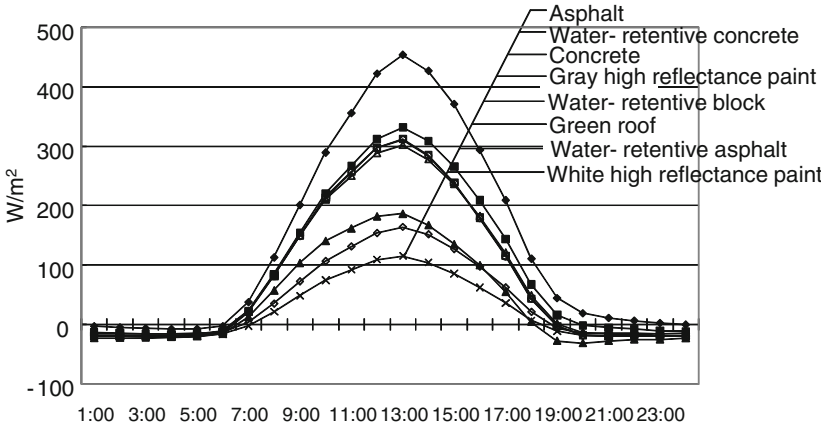


Fig. 1.29 Average sensible heat flux from various surfaces during the summer period of 2005

each technology is judged to be good. On the other hand, the effects of the energy saving by these technologies are not much larger than those from insulation; therefore, insulation has priority over cool roofs and green roofs in the event that energy saving is made a top priority. For additional information, other effects and matters taken into consideration are also shown in Table 1.1. The maintenance of green roofs and age-related deterioration (solar reflectance) of cool roofs is an important matter for consideration. Green roofs provide a variety of benefits such as improving the landscape, ecosystem, real estate values, etc.; therefore, green roofs are different from cool roofs as we know what benefits to expect. On the basis of these characteristics, however, it is expected that the appropriate technical choice takes the local climate or building use into consideration.

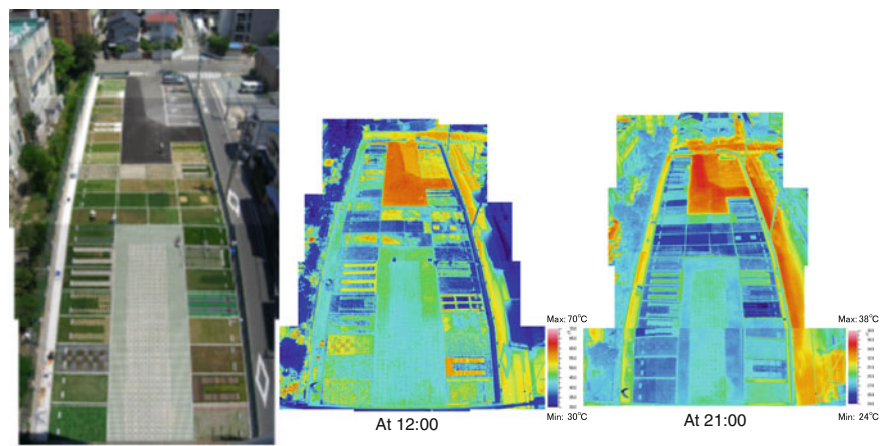


Fig. 1.30 Surface heat budget experiments on parking lots and thermal images

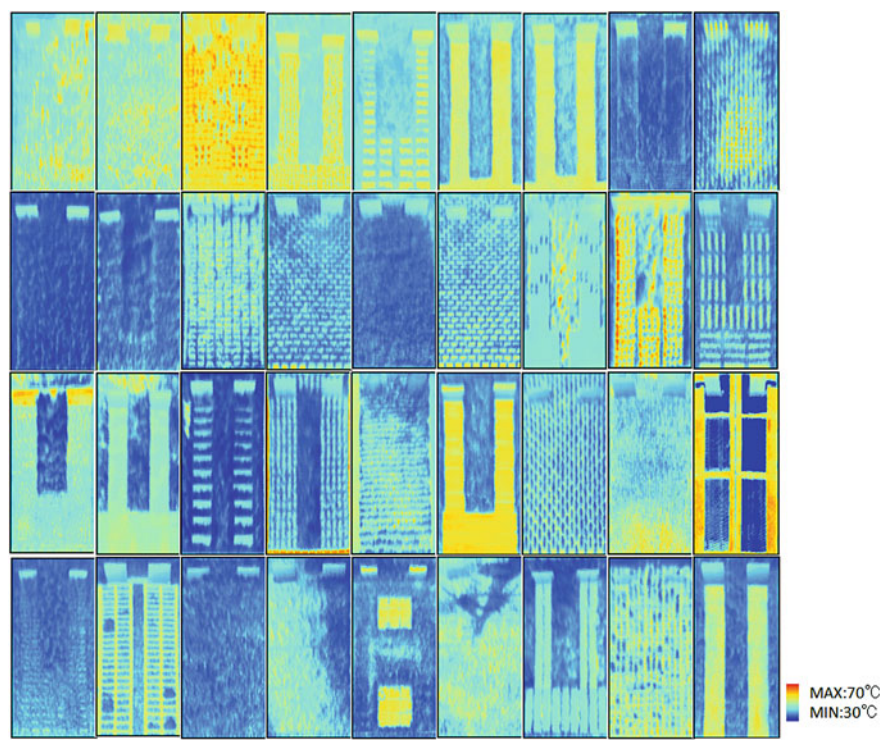


Fig. 1.31 Observation results of surface temperature at 12:00, August 20, 2005

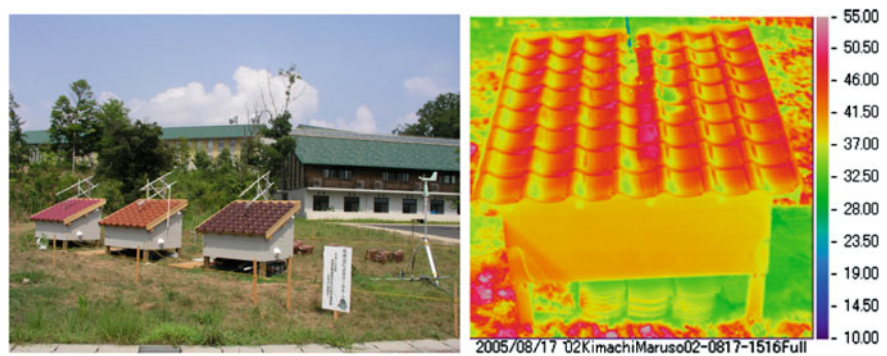


Fig. 1.32 Surface heat budget experiments on tile roofs and thermal images

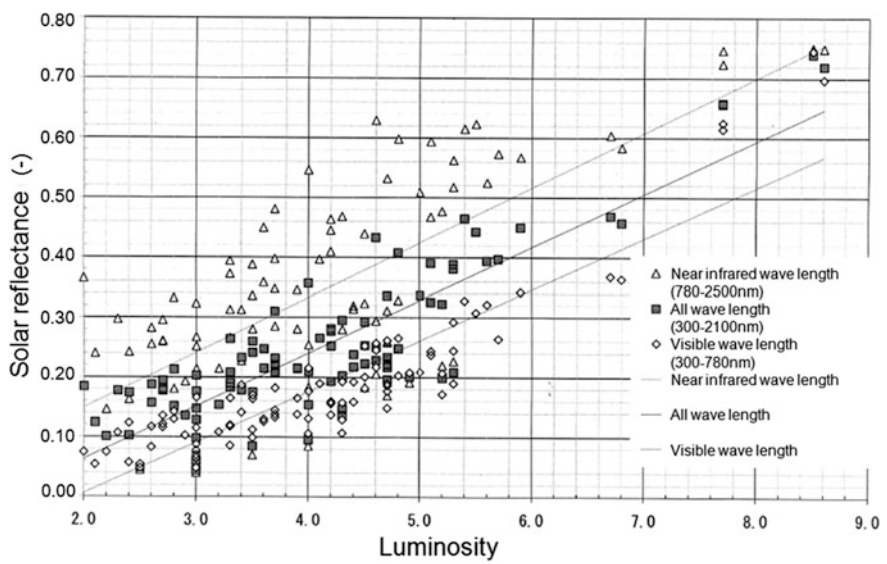


Fig. 1.33 Relationship between luminosity and solar reflectance of traditional Japanese roof tiles



Fig. 1.34 View factors of each surface of typical Japanese roof tiles

Table 1.1 Summary of the effect of urban heat island measure technologies on surface heat budget

Target	Menu	Heat island measures		Improvement of outdoor thermal		Energy saving		Other effects	Consideration matters
		Day time	Night time	Day time	Night time	Cooling	Heating		
Roof	High reflectance	⊙	⊙	-	-	○	△	Improvement of indoor thermal environemt, Non-increase of humidity	Attention to the aging of the performance Consideration to the reflected solar radiation Heating load increases
	Green	⊙	⊙	⊙ (roof)	⊙ (roof)	○	○	Improvement of landscape, Attract customers, Mitigation of urban flooding, Conservation of the ecosystem, Environmental education, Improvement of real estate value	Appropriate maintenance
	Evaporation	⊙	○	-	-	○		Rainwater penetration	Water way measures Maintenance of water retention performance Note the degradation due to freeze-thaw
Wall	Green	⊙	○	⊙ (street)	⊙ (street)	○	○	Improvement of landscape, Conservation of ecosystem	Appropriate maintenance
	Evaporation	⊙	○	○	-	○	-	Improvement of landscape, Rainwater penetration	Water way measures Maintenance of water retention performance Note the degradation due to freeze-thaw
Road, Pavement, Parking, Open space	High reflectance	⊙	⊙	△	⊙	-	-	Non-increase of humidity	Attention to the aging of the performance Consideration to the reflected solar radiation
	Green	⊙	⊙	⊙	⊙	-	-	Improvement of landscape, Conservation of ecosystem	Appropriate maintenance
	Evaporation	⊙	⊙	⊙	⊙	-	-	Rainwater penetration	Maintenance of water retention performance Note the degradation due to freeze-thaw

⊙: Superior effect is expected, ○: Good effect is expected, △: Opposite effect may occur, -: Not intended

1.2.4 Appropriate Selection of Urban Heat Island Measure Techniques

1.2.4.1 Evaluation of the Effective Temperature of the Human Body [10]

Environmental elements affecting the effective temperature of the human body are shown in Fig. 1.35. Certain factors affect the human body making people feel warm, such as high levels of incident solar radiation, high levels of radiation from roads and building surfaces, high air temperatures, high humidity and low wind velocity, high metabolic rates after exercise or working, and wearing many clothes. The standard new effective temperature (SET) and wet bulb globe temperature (WBGT) are generally used as indicators of effective temperature in outdoor spaces.

Fig. 1.35 Environmental elements affecting the effective temperature of the human body

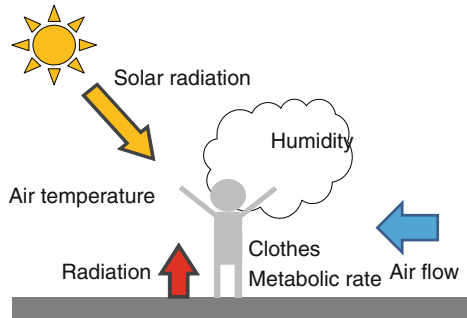


Fig. 1.36 Relationship between SET* and comfortable sensation

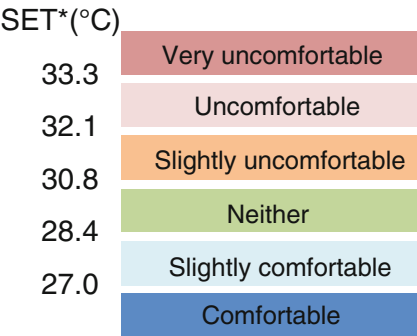
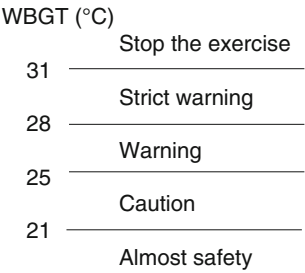
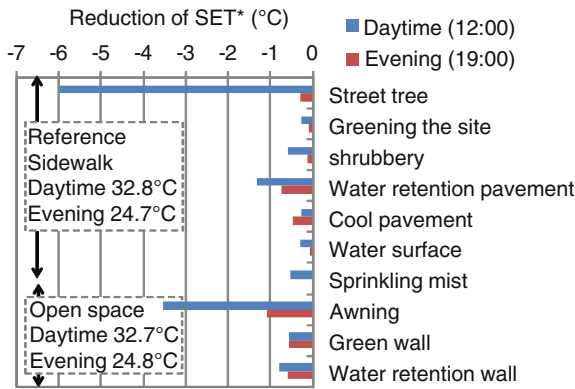


Fig. 1.37 Guidelines for exercise in outdoor spaces for each WBGT



The relationship between SET and comfort sensations is shown in Fig. 1.36. Guidelines for exercising in outdoor spaces for each WBGT are shown in Fig. 1.37. When high temperatures are indicated, people feel warm. Furthermore, very high temperatures have a worse effect on the body and may cause heat stroke. Various measures to reduce SET are shown in Fig. 1.38. The shade from street trees and awnings has a large effect on reducing incident solar radiation to the human body. Reducing incident solar radiation is more effective to human thermal sensation than

Fig. 1.38 Reduction of SET* by various measures



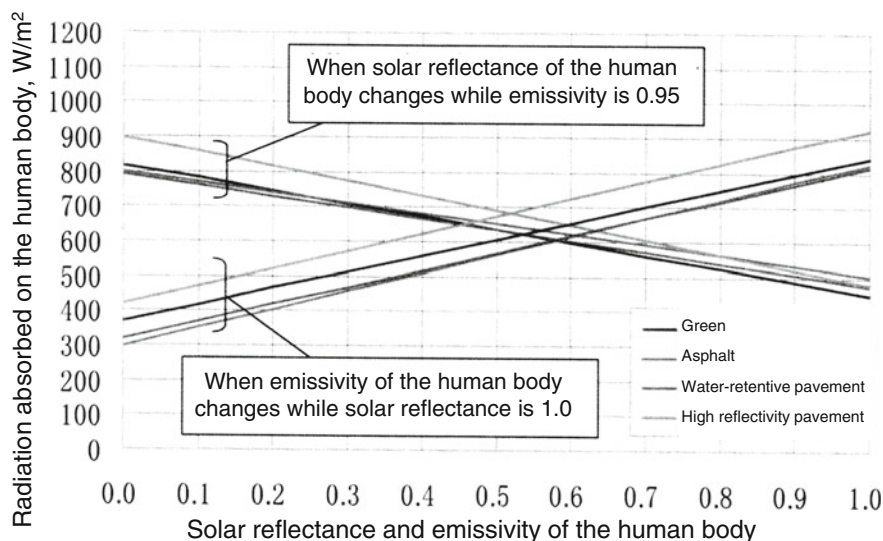


Fig. 1.39 Radiation absorbed by the human body by changes in solar reflectance and emissivity

reducing surface temperature on roads and wall using green and water-retentive materials. It is especially important for improving human thermal sensation in outdoor spaces.

To reduce incident solar radiation, it is important to adjust the solar reflectance and emissivity of the human body. Radiation absorbed by the human body by changes in solar reflectance and emissivity is shown in Fig. 1.39. Radiation absorbed by the human body decreases when solar reflectance by the human body increases (white clothes) or emissivity of the human body decreases (metal clothes). Evaluation results on green, asphalt, water-retentive pavements, and high-reflectance pavements are also shown in Fig. 1.39. Radiation absorbed by the human body on green, water-retentive pavements, high-reflectance pavements is small, approximately $100 W/m^2$ less than on asphalt. However, radiation absorbed by the human body with white clothes is even smaller, approximately $300 W/m^2$ less than with black clothes. Therefore, it is more effective to wear white clothes than to change ground surface cover for human thermal sensation.

1.2.4.2 Appropriate Selection of Urban Heat Island Measure Techniques on Urban Streets [11]

As heat island countermeasures on urban streets have the second highest priority, the daily average surface temperature reduction caused by street trees is shown in Fig. 1.40. The greatest benefits are observed on the northern sidewalk of the east-west road and the eastern and western sidewalk of the north-south road area.

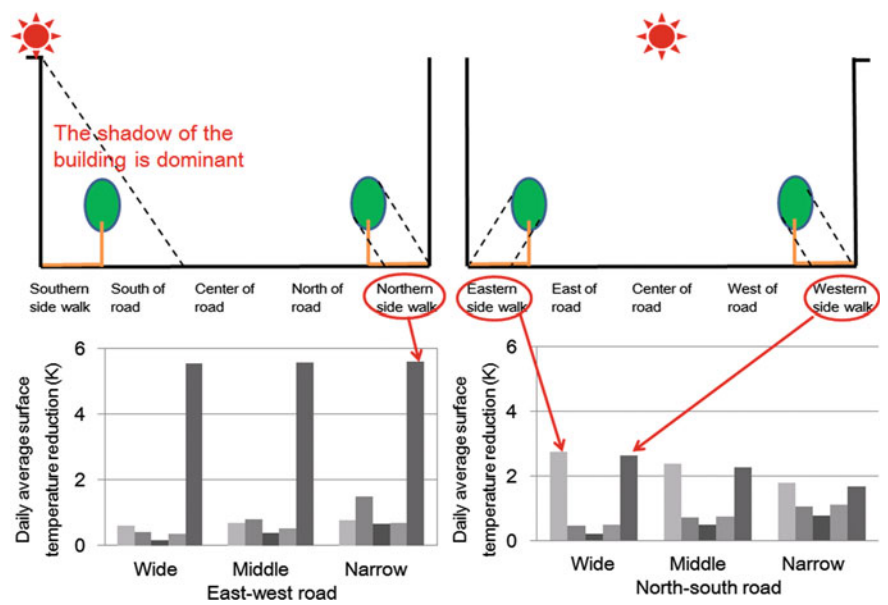


Fig. 1.40 Daily average surface temperature reductions due to street trees (*left*, east–west road; *right*, north–south road)

The reduction in daily average surface temperatures due to high-reflectance paint is shown in Fig. 1.41. The benefits are greater at the center of the north–south road and from the center to the northern side of the east–west road, where the solar radiation gain is large. The difference in benefits due to water-retentive pavements and high-reflectance paint depends on the evaporation efficiency of the water-retentive pavements, the solar reflectance of the high-reflectance paint, and weather conditions.

The benefits from both high-reflectance paint and water-retentive pavements appear mainly on the roadway. On the other hand, the benefit from street trees is concentrated mainly on the sidewalk. This is because the benefit from street trees is caused by the tree crown shielding the solar radiation, and their shadows occur mainly on the sidewalk. Therefore, it can be inferred that the introduction of water-retentive pavements and high-reflectance paint on the roads is more appropriate for reducing road surface temperatures, while the introduction of roadside trees is more appropriate for improving the thermal environment of the sidewalk. Technology such as wall-based solar radiation shielding (e.g., green walls) is suitable for reducing the temperature of wall surfaces.

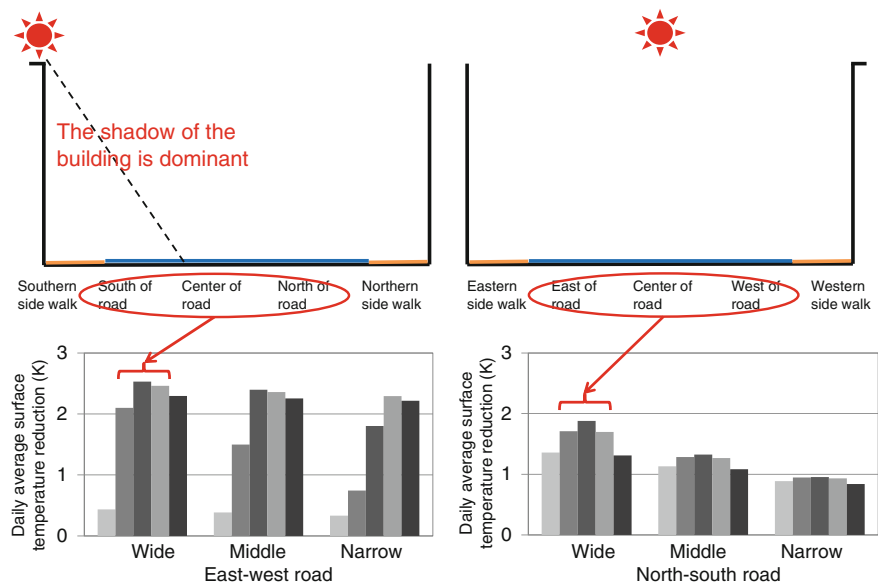


Fig. 1.41 Daily average surface temperature reductions due to high-reflectance paint (*left*, east–west road; *right*, north–south road)

1.2.4.3 Layout of Street Trees [11]

The average mean radiant temperature (MRT) along a street at 15:00 at various tree intervals is shown in Fig. 1.42. The tree crown width is set at 4 m. As pedestrians tend to walk on the center of the sidewalks, the MRT that represents the thermal environment for pedestrians is averaged along the sidewalk. The influence of the reduction in short-wave (solar) radiation gain is significant for MRT. The influence of the difference in layout of the street trees is mainly due to the difference in short-wave radiation falling on the human body. The reduction in MRT is greater on the northern sidewalk of the east–west road than on the eastern sidewalk of the north–south road. Because the shadows of the roadside trees fall in a direction perpendicular to the eastern sidewalk of the north–south road and in a direction parallel to the northern sidewalk of the east–west road, there is a large area where the human body is under the influence of a shadow on the northern sidewalk of the east–west road.

The reduction in MRT on the sidewalk depends on the area where the human body is under the influence of a shadow. The shadow tends to fall in a direction perpendicular to the eastern sidewalk of the north–south road and in a direction parallel to the northern sidewalk of the east–west road. Therefore, the shadow area on the northern sidewalk of the east–west road is larger than on the eastern (western) sidewalk of the north–south road.

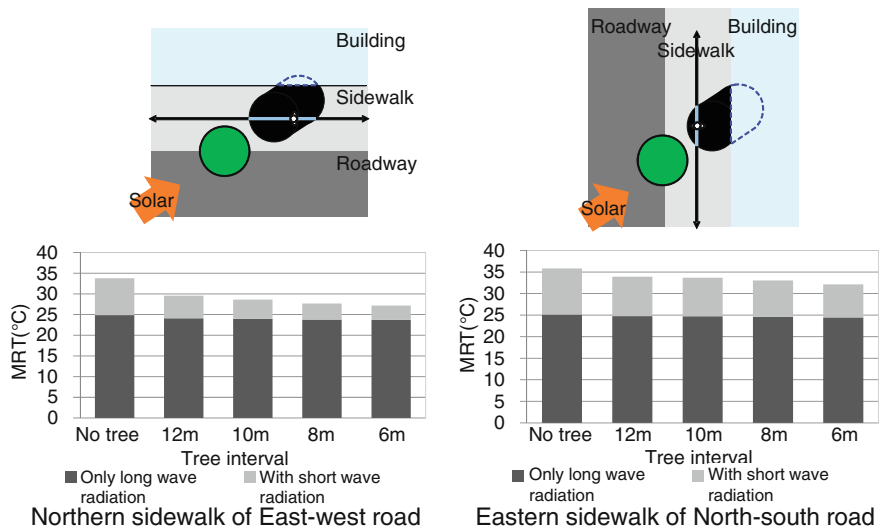


Fig. 1.42 MRT averaged along a street at 15:00 at various tree intervals (crown width is 4 m) (*left*, northern sidewalk of the east–west road; *right*, eastern sidewalk of the north–south road)

1.3 Reduction of Exhaust Heat

Measures for reducing exhaust heat released from outdoor units of air conditioners include reducing the cooling load of a room and improving heat release methods. The relationship between cooling load and exhaust heat released from outdoor units of air conditioners, and release method is shown in Fig. 1.43.

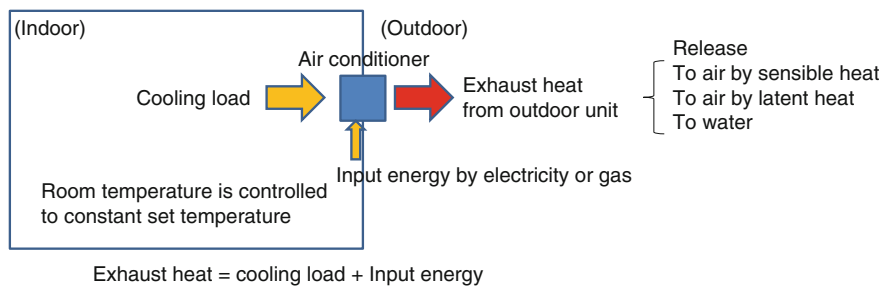


Fig. 1.43 Relationship between cooling load and exhaust heat released from outdoor units of air conditioners, and release method

1.3.1 Reduction of Cooling Load

Heat pump air conditioners, which are generally used in homes, supply cold air to the room by discharging warm air from the outdoor units to the outdoor spaces. If a large amount of cold air is required in the room, a large amount of warm air from the outdoor unit is required. It is called anthropogenic heat release, and is the cause of urban heat island. Therefore, reducing the amount of cold air required in a room, i.e., reducing the cooling load, results in a reduction of anthropogenic heat release. The main factors that influence the cooling load are the heat generated from equipment and human bodies in the room and the amount of heat coming from outside through the windows, walls and by the ventilation. Various energy saving strategies have been proposed. In addition, if the cold air is generated by lower input energy (electricity and gas), anthropogenic heat release from the outdoor units is reduced (high-efficiency equipment).

1.3.2 Improving the Heat Release Method

Anthropogenic heat released to the atmosphere contributes to a rise in air temperature, which is combined with sensible heat from roofs, walls and road surfaces. Improving the release method of anthropogenic heat so as not to contribute to a rise in air temperature is one of the heat island measures. Specifically, the anthropogenic heat released from the outdoor units is released into the sewerage, water supplies, and industrial water supplies which are existing infrastructure, or into rivers, sea, groundwater, and underground aquifers which contain natural water, taking into consideration that a rise in water temperature due to anthropogenic heat release will not have a negative impact on human health and ecosystems.

If the anthropogenic heat from outdoor units is released into the atmosphere from high places such as roofs, the rise in air temperature is mitigated by the diffusion effect of the upper air. If water is sprayed at the outlet of the outdoor units, the evaporation heat is deprived by evaporation of the water, and the air temperature of the exhaust heat is lowered. It is thought that approximately 40 % of sensible heat is converted to latent heat [12]. A similar principle is to use cooling towers instead of outdoor units to reduce the percentage of sensible heat that affects rising air temperatures. Figure 1.45 shows the behavior of a cooling tower on a psychrometric chart [13]. A photograph of a cooling tower is shown in Fig. 1.44. Enthalpy (constituted by latent and sensible heat) released to the outside air depends on the internal cooling load. When the cooling load is small the enthalpy is released only by latent heat release; as a result, the dry-bulb temperature does not rise but white absolute humidity rises. However, when the cooling load is large the enthalpy is released by both latent and sensible heat release; as a result, both dry-bulb temperature and absolute humidity rise. It is thought that approximately 90 % of the sensible heat is converted to latent heat. If heat is supplied to a building by a heat pump water supplier, cold air is released into the atmosphere from the outdoor unit,



Fig. 1.44 Photograph of a cooling tower

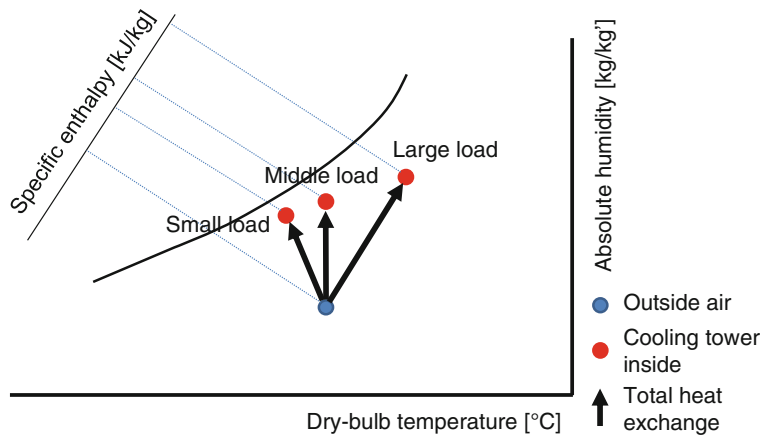


Fig. 1.45 Psychrometric chart showing the behavior of a cooling tower

and the heat island measure effect occurs. As there is a relatively large hot water supply load in restaurants, hotels, and sports facilities in the summer, the heat island measure effect is expected locally. Simulation results of air temperature distribution when outdoor units for hot water supplies and air conditioners are installed in tenement residential areas are shown in Fig. 1.46 [14]. Since street widths are narrow, the effects of hot and cold air released from the outdoor units are relatively large. If the outdoor units are installed in places with poor ventilation, it is necessary to consider preventing high temperatures locally.

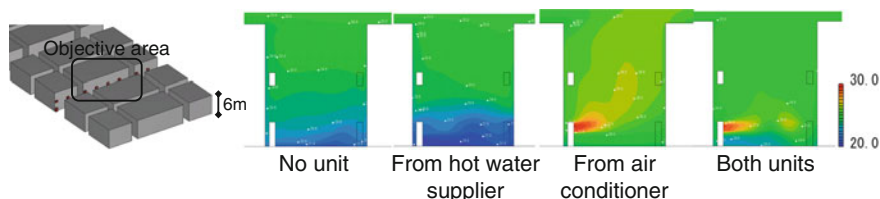


Fig. 1.46 Simulation results of air temperature distribution when the outdoor units of hot water suppliers and air conditioners are installed in tenement residential areas with a 5-m street width

1.4 Improving Ventilation

If the sensible heat flux from surfaces with higher temperatures such as roofs, walls and roads or anthropogenic heat release from the outdoor units of heat pumps stays in the near ground surface, the air temperature near the ground surface will rise. Therefore, preventing heat retention by improving the ventilation near the ground surface is one of the heat island measures.

In this situation, synoptic wind is weak when the thermal environment worsens. Available climate resources are land and sea breezes blowing in response to the temperature difference between the land and sea, the mountain and valley winds blowing on the slopes of mountains, the cold air drainage flowing down the slopes, and the cool air flowing from the parks and green areas.

To make use of these climate resources effectively, it is important to prepare the building geometry status in urban areas.

1.4.1 Wind as a Climate Resource

1.4.1.1 Land and Sea Breezes

Many of the large cities in Japan face the sea and, as a result, they have benefited from the air temperature mitigation effect of the sea breeze. Distance from the sea and mean air temperatures are shown in Fig. 1.47 [15]. Air temperatures near the coast are lower by approximately 3 K than inland, and are dominated by sea breezes during the day time. Air temperatures near the coast do not decrease so much during the night due to the heat capacity of the sea. However, inland air temperatures stay high due to the effects of urbanization, and land breezes are lighter. Built-up areas near the coast are useful for evaluating the cooling effects of sea breezes.

If the cooling potential from sea breezes is used in windward urban areas, the potential is reduced and the air temperature may rise in leeward urban areas. Urban forms and the use of cold air by sea breeze are shown in Fig. 1.48 [16]. It is necessary to consider whether the distribution of cold air by sea breeze is more reasonable and fair.

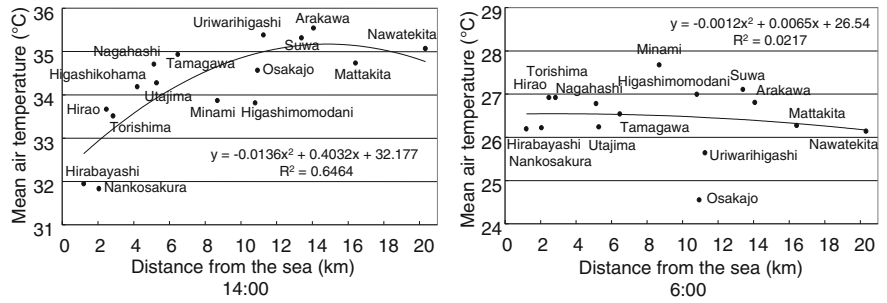
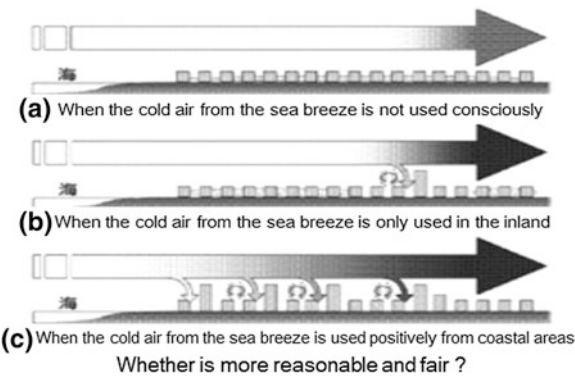


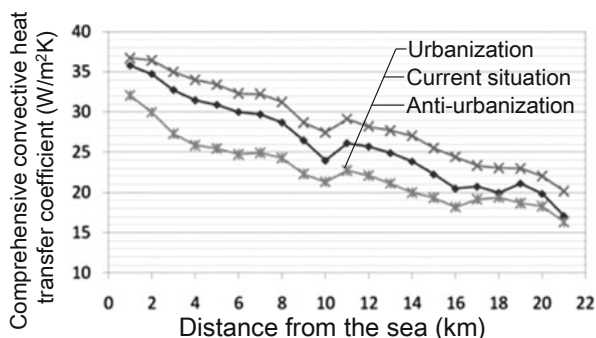
Fig. 1.47 Distance from the sea and average mean air temperature in August 2000 (*left*, 14:00; *right*, 6:00)

Fig. 1.48 Urban forms and the use of cold air by sea breezes



The calculation results of comprehensive convective heat transfer coefficient by WRF, the mesoscale weather simulation model, on a typical fine summer day is shown in Fig. 1.49 [17]. The comprehensive convective heat transfer coefficient rises with the increase of upper wind velocity when the sea breeze enters inland areas. As a result, sensible heat flux transported to the upper air increases, keeping the air temperature near the ground low; this is caused by air temperature mitigation due to the sea breeze. In other words, the anthropogenic heat release from air conditioning outdoor units and sensible heat flux from the buildings and ground surface tend to mix with the upper air in conditions dominated by the sea breeze; therefore, the air temperature near the ground does not rise. Figure 1.49 shows the reduction of comprehensive convective heat transfer coefficient due to urbanization to be approximately 3 W/(m² K), and the reduction at a distance of 10 km from the sea to be approximately 10 W/(m² K). The effect of the distance from the sea is more dominant than the effect from urbanization. Therefore, the effects on leeward built-up areas by windward built-up areas are not so large.

Fig. 1.49 Calculation results of comprehensive convective heat transfer coefficient by WRF, the mesoscale weather simulation model, on a typical fine summer day



1.4.1.2 Mountain and Valley Winds

During the night, surface temperatures in both built-up and natural areas decline by radiative cooling; however, surface temperatures on cement and asphalt concrete stay high due to their large heat capacity in built-up areas. Since cold air generated by radiative cooling is relatively heavy, it flows downstream along the slope. Calculation results of cold air drainage in the Kobe area are shown in Fig. 1.50 [18]. Cold air flows down along the slope and accumulates in the valley, before flowing out to the built-up areas. The built-up areas benefit from the cooling effects of cold air drainage from the valleys. Since the built-up areas of Kobe city face Mount Rokko, it is necessary to take the effective use of cold air drainage into consideration.

Observation results of wind direction frequency and air temperature in weak and strong winds are shown in Fig. 1.51. The dominant wind direction is from the valley; however, the directions of both land and sea breezes have been confirmed in the built-up area. When the wind is weak, the cold air flows into the built-up area gradually and the air temperature at the point close to the valley is relatively lowered. On the other hand, when the wind is strong, air temperatures in the built-up area are almost similar due to the dominating land and sea breezes. Therefore, it is necessary to investigate the occurrence frequency of these phenomena when considering the effective use of cold air drainage.

Observed and calculated results of air temperature distribution in the residential area facing the mouth of the valley are shown in Fig. 1.52 [19]. Air temperature falls in the riverside area and stays high in the southern built-up area; this is due to the heat exchange between the cold air from the valley and the buildings and road surfaces, depending on the distribution of surface temperatures and roughness parameters.

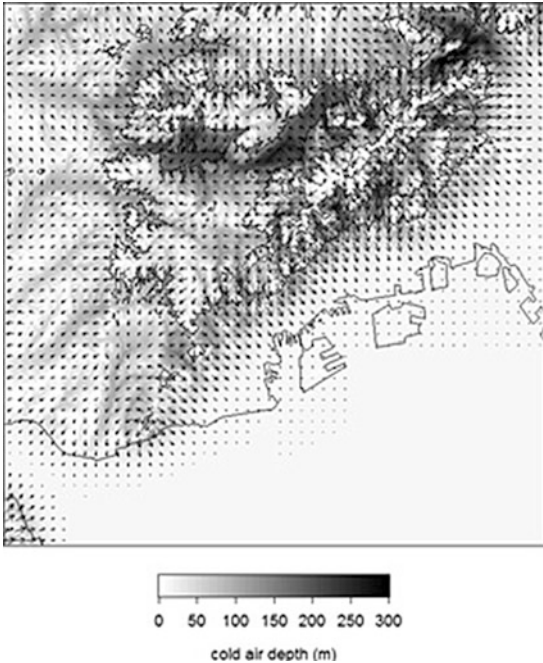


Fig. 1.50 Calculation results of cold air drainage in the Kobe area

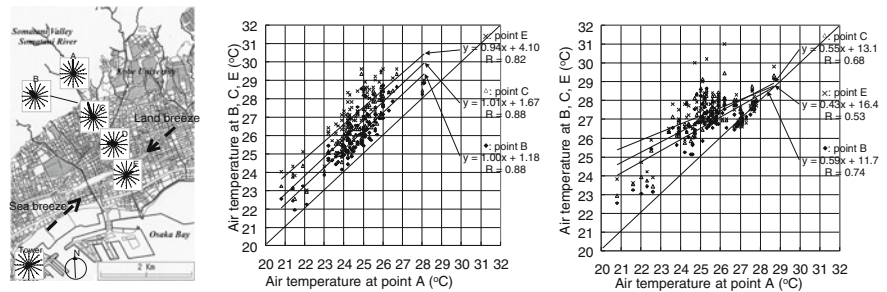


Fig. 1.51 Observation results of wind direction frequency (left), and air temperature in weak wind (center) and strong wind (right) on a summer night in the urban area on the southern side of Mount Rokko

1.4.1.3 Cold Air Drainage from Parks [20]

Air temperatures during the night in parks and green areas decrease due to radiative cooling and are approximately 1–2 K less than in built-up areas with a large thermal capacity. When the wind is weak, cold air flows into the built-up areas as a density flow based on air temperature difference between the parks and built-up areas.

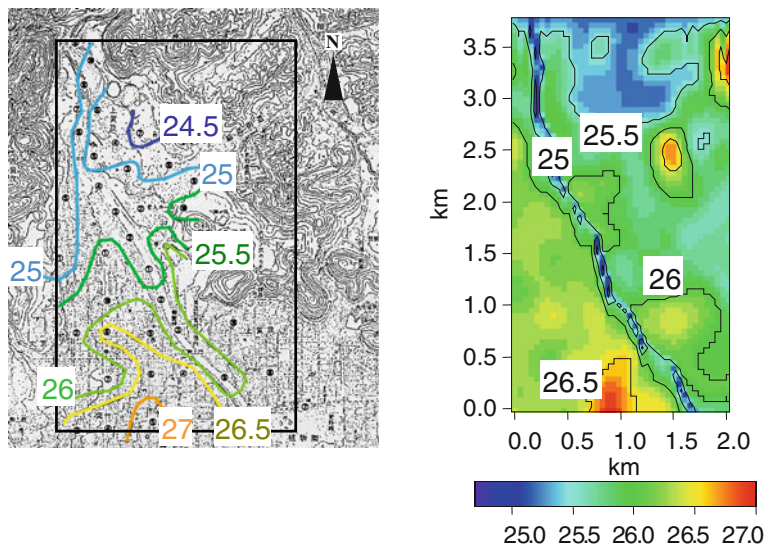


Fig. 1.52 Observed and calculated results of air temperature distribution in the residential area facing the mouth of the valley at 1:00 on August 9, 2001

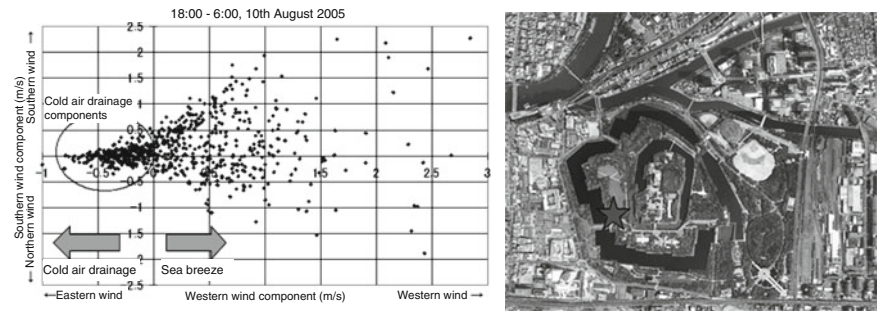


Fig. 1.53 Observation results of cold air drainage from Osaka Castle Park (*star*, observation point)

Observation results of cold air drainage from Osaka Castle Park are shown in Fig. 1.53. Cold air drainage has not been confirmed when western winds blow in this area, but has been confirmed when synoptic winds are weak. Cold air drainage with a velocity below 0.5 m/s flows out from Osaka Castle Park to western built-up areas. During this time, the air temperature in the built-up areas may decrease approximately 2–3 K; this phenomenon occurs only on a calm fine night.

Observation results of air temperature and wind velocity and direction in and around Daisen Park are shown in Fig. 1.54. Air temperature falls approximately 1–2 K at 23:00 to 0:00 when wind direction changes from west to east, and wind velocity is less than 0.5 m/s. Air temperature rises after 0:00 with a relatively large

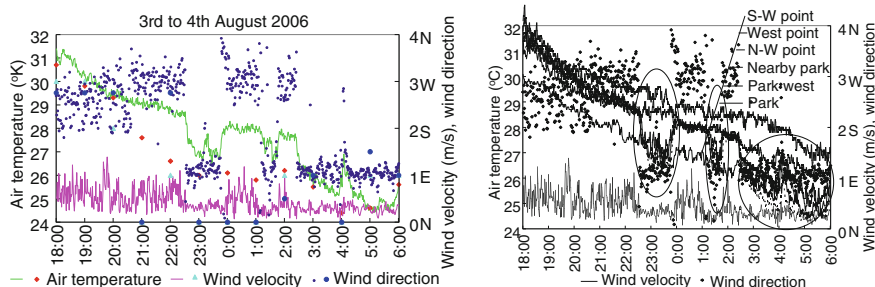


Fig. 1.54 Observation results of air temperature and wind velocity and direction in and around Daisen Park

wind velocity in a western direction. Large temperature falls are then confirmed after 1:00 and after 3:00 when the changes in wind velocity and direction are similar to the previous change. The air temperature at different observation points around the park also decreases in synchronization with air temperature changes in the park; however, there are no changes in the air temperature at any of the different observation points in the built-up areas. Although all the observation points are located approximately 100 m from the park, the areas affected by cold air drainage are limited by the urban block form, and building shape, etc.

1.4.2 Ventilation in Street Canyons [21]

To make effective use of the cooling and ventilating effects of the wind as a climate resource, it is necessary to prepare the building geometry status of the urban areas. Generally, since resistance to wind is increased by urbanization, the wind environment in the built-up areas becomes worse. Suppressing the building coverage ratio leads to an improvement in ventilation in street canyons.

Calculation results of wind velocity distribution in Osaka City are shown in Fig. 1.55. Individual building shape data handled by a Geographic Information Systems (GIS) is provided by Osaka city office. Wind velocity is greater in open spaces such as sea, rivers and large parks and smaller where buildings are built up densely, particularly within Osaka. The relationship between mean wind velocity and urban block component ratio in a 500-m square grid is shown in Fig. 1.56; in this instance, the mean wind velocity is determined better by open space ratio rather than by gross building coverage ratio.

The relationship between mean wind velocity and urban block component ratio in a 500-m square grid is shown in Fig. 1.57; in this instance the gross building coverage ratio is less than 30 %, and mean wind velocity is decreased due to increased gross building coverage ratio. When the gross building coverage ratio is more than 30 %, the mean wind velocity is almost constant. The relationship

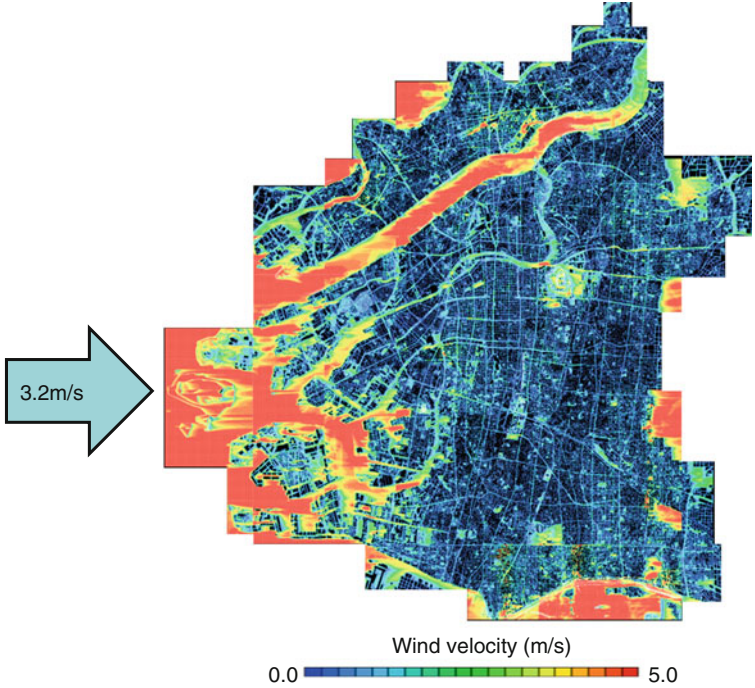


Fig. 1.55 Calculation results of wind velocity distribution in Osaka City

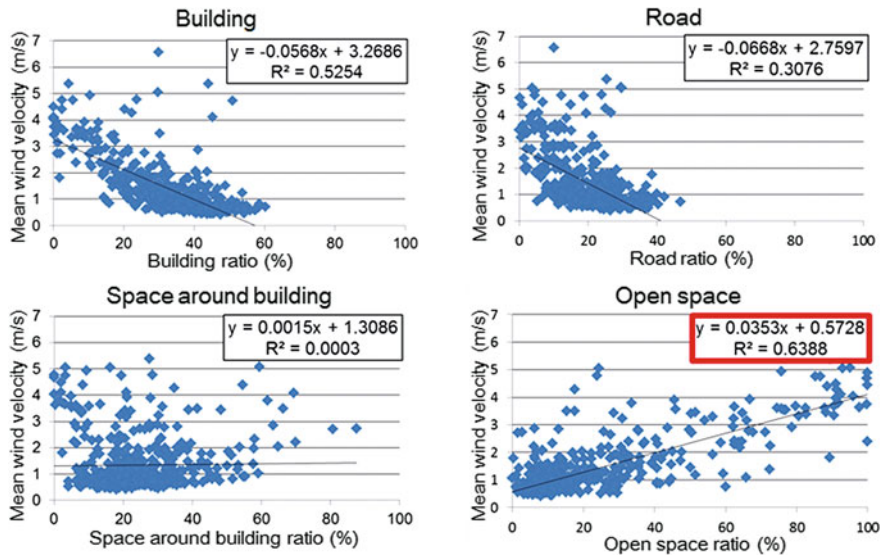
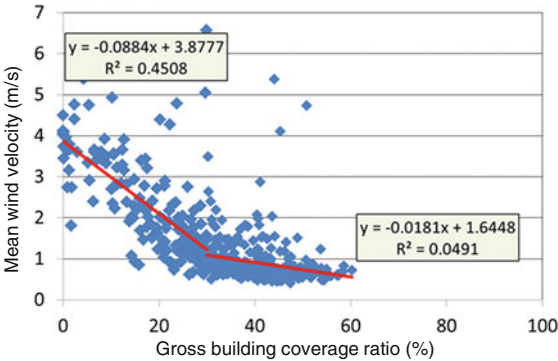


Fig. 1.56 Relationship between mean wind velocity and the urban block component ratio in a 500-m square grid

Fig. 1.57 Relationship between the gross building ratio and mean wind velocity in a 500-m square grid



between gross building coverage ratio and urban block component ratio in a 500-m square grid is shown in Fig. 1.58; in this instance, the gross building coverage ratio is more than 30 %, and the open space ratio is almost constant. Therefore, mean wind velocity is almost constant. To summarize, the mean wind velocity averaged in a 500-m square grid is influenced by the open space ratio more than by the gross building coverage ratio.

The relationship between road width and wind velocity ratio to the upper wind is shown in Fig. 1.59. Ventilation in street canyons is improved on wider roads parallel to the main wind direction. The relationship between mean building height and wind velocity ratio to upper winds is shown in Fig. 1.60. Building arrangements are shown in Fig. 1.61. If there is a variation in a perpendicular or staggered arrangement of building heights in the target area, ventilation in the street canyons is improved even if the mean building height is low. The influence of building height in windward areas on the wind velocity in street canyons is not so large.

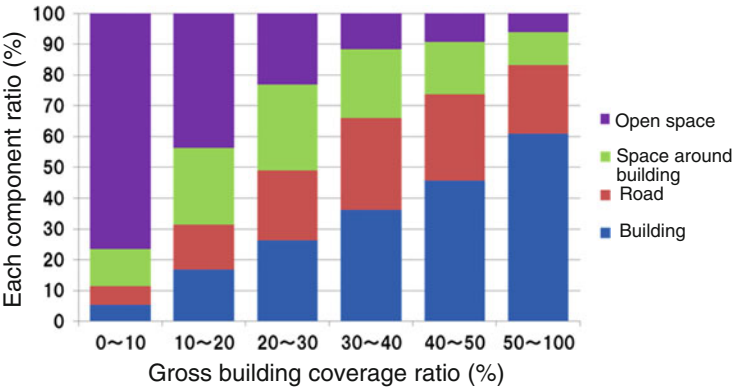


Fig. 1.58 Relationship between the gross building coverage ratio and urban block component ratio in a 500-m square grid

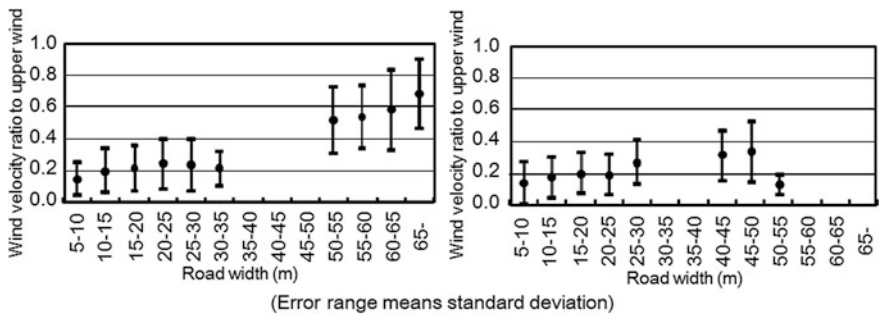


Fig. 1.59 Relationship between road width and wind velocity ratio to upper winds (*left*, on the road parallel to the main wind direction; *right*, on the road perpendicular to the main wind direction)

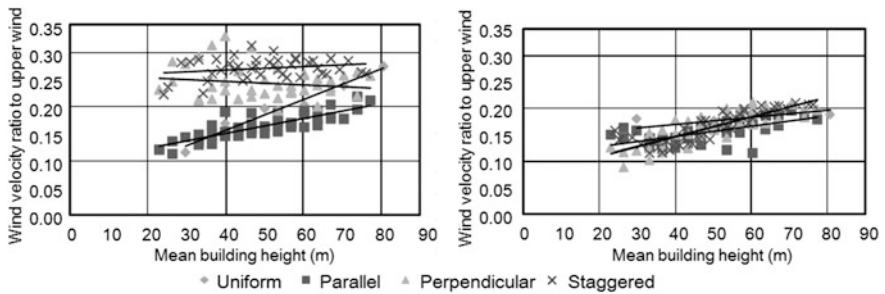


Fig. 1.60 Relationship between mean building height and wind velocity ratio to upper winds (*left*, where building height in the target area changes; *right*, where building height in windward areas changes)

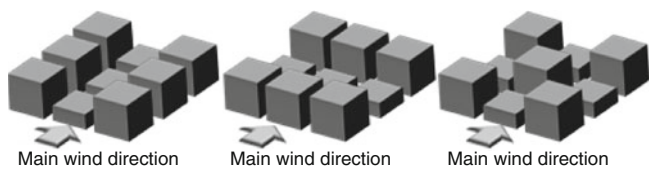


Fig. 1.61 Buildings arrangements (*left*, parallel arrangement; *center*, perpendicular arrangement; *right*, staggered arrangement)

1.5 Conclusions

Specific measures for the urban heat island phenomenon are summarized in the following three points.

- Improving surface cover
- Reducing exhaust heat
- Improving ventilation

The urban heat budget model is used for calculating air temperature near the ground surface. Since sensible heat flux from urban areas is larger than from natural areas due to the small amount of natural land cover area, the air temperature in urban areas is higher than in natural areas.

With regard to improving surface cover, the appropriate heat island measure techniques on surface cover, i.e., cool roofs, green roofs, and cool pavements, etc., should be preferentially introduced to places where the surface temperatures tend to rise. Places where surface temperatures tend to rise, i.e., roofs, northern side of east–west roads, and center of north–south road, are identified on the basis of the relationship between street canyon characteristics and solar radiation gain. The most effective measure techniques should be selected for the target place; these should be determined by predicting the effect by each technique, as far as possible. The effects of urban heat island measure techniques on surface cover are evaluated by surface heat budget on each surface and by solar radiation shielding effects by street trees.

With regard to reducing exhaust heat, measures for reducing exhaust heat released from the outdoor units of air conditioners are the reduction of cooling loads in rooms and improving heat release methods. The main factors affecting the cooling loads are the heat generated from equipment and human bodies in the rooms and the heat coming from outside through the windows, walls and by ventilation. Various energy saving strategies have been proposed. Improving the release method of anthropogenic heat so as not to contribute to rises in the air temperature is one of the heat island measures. Specific measures for reducing exhaust heat are releasing anthropogenic heat into the existing infrastructure or natural water, releasing anthropogenic heat from high places such as roofs, water sprays at the outlet of the outdoor units, the use of cooling towers, and the use of heat pump water suppliers, etc.

With regard to improving ventilation, preventing heat staying in the street canyons by improving ventilation near the ground surface is one of the heat island measures. Land and sea breezes, mountain and valley winds, cold air drainage flowing down the slope, and cool air flowing from the parks and green areas are available climate resources. To make use of these climate resources effectively, it is important to prepare the building geometry in urban areas. Generally, since the resistance to wind is increased by urbanization, the wind environment in the built-up areas becomes worse. Suppressing the building coverage ratio leads to improvements in ventilation in street canyons. The relationship between ventilation in street canyons and urban block morphology is analyzed based on the results of computational fluid dynamic calculations. Ventilation in street canyons is improved on wider roads parallel to the main wind direction. If there is a variation of building heights in a perpendicular or staggered arrangement in the target area, the ventilation in street canyons is improved even if the mean building height is low.

References

1. H. Takebayashi, Y. Kondo, WG for the appropriate use of cool roof of AIJ, Development of evaluation tool for public benefit, Simple evaluation system of cool roof for proper promotion (Part 2), AIJ J. Technol. Des., 33, 589–594, 2010 (in Japanese with English abstract)
2. Ministry of the Environment of Japan, Study report of heat island countermeasure technique in FY 2001, 2002, <https://www.env.go.jp/air/report/h14-02/index.html> (in Japanese)
3. H. Takebayashi, M. Moriyama, Study on a simple evaluation method of urban heat island mitigation technology using upper air data, Journal of heat island institute international, 7(2), 102–110, 2012
4. H. Takebayashi, M. Moriyama, Relationships between the properties of an urban street canyon and its radiant environment: Introduction of appropriate urban heat island mitigation technologies, Solar Energy, 86(9), 2255–2262, 2012
5. H. Takebayashi, M. Moriyama, Surface heat budget on green roof and high reflection roof for mitigation of urban heat island, Building and Environment, 42, 2971–2979, 2007
6. H. Takebayashi, M. Moriyama, Study on surface heat budget of various pavements for urban heat island mitigation, Advances in Materials Science and Engineering, 2012
7. H. Takebayashi, M. Moriyama, Study on the urban heat island mitigation effect achieved by converting to grass-covered parking, Solar Energy, 83(8), 1211–1223, 2009
8. H. Takebayashi, M. Moriyama, T. Sugihara, Study on the cool roof effect of Japanese traditional tiled roof: Numerical analysis of solar reflectance of unevenness tiled surface and heat budget of typical tiled roof system, Energy and Buildings, 55, 77–84, 2012
9. Architectural Institute of Japan, Cool roof guidebook, Technology to cool the city, Chijinskyokan, 2014
10. Ministry of the Environment of Japan, Heat island measures manual, Recent status and Toward the spread of adaptation measures, 2012, http://www.env.go.jp/air/life/heat_island/manual_01.html (in Japanese)
11. H. Takebayashi, Y. Kimura, S. Kyogoku, Study on the appropriate selection of urban heat island measure technologies to urban block properties, Sustainable Cities and Society, 13, 217–222, 2014
12. The society of heating, air-conditioning and sanitary engineers of Japan, Heat island measures, way of thinking and how to proceed for urban normal temperature planning, Ohmsha, 2009
13. N. Yoshida, W. Fukuyori, H. Takebayashi, E. Ishii, M. Kasahara, S. Tanabe, M. Kouyama, Study on performance evaluation of the heat island measures technology in composite facilities, Part 2 Evaluation of latent heat release of the cooling tower based on the observation, Proc. Academic research conference of Kinki chapter of the society of heating, air-conditioning and sanitary engineers of Japan, 43, 5–8, 2014
14. H. Takebayashi, M. Moriyama, M. Kasahara, Study on mitigation of outdoor thermal environment by the unit of heat pump water supply, Transactions of the Society of Heating, Air-Conditioning and Sanitary Engineers of Japan, 145, 1–7, 2009 (in Japanese with English abstract)

15. H. Takebayashi, M. Moriyama, Urban heat island phenomena influenced by sea breeze, *AJ J. Technol. Des.*, 21, 199–202, 2005 (in Japanese with English abstract)
16. A. Mochida, Y. Ishida, ‘Kazenomichi’ (wind path), *Tenki*, 56, 571–572, 2009
17. T. Kishimoto, H. Takebayashi, M. Moriyama, Study on the urban climate influenced by sea breeze using WRF model and upper weather data over the city, *Proc. The 6th Japanese-German Meeting on Urban Climatology*, 2012
18. H. Takebayashi, M. Moriyama, Cooling effects on a built-up area caused by cold air drainage in summer night, *Proc. 3rd Japanese-German Symposium on Urban Climatology*, pp. 24–25, 2000
19. H. Takebayashi, M. Moriyama, Improvement of outdoor thermal environment using cold air drainage in a built-up area facing the mouth of a valley, *Proc. Fifth International Conference on Urban Climate*, 2003
20. H. Takebayashi, M. Moriyama, Analysis of cold air drainage from the park in urban area by observations, *Journal of Heat Island Institute international*, 3, 34–39, 2008 (in Japanese with English abstract)
21. H. Takebayashi, M. Moriyama, The evaluation of the introduction effect of urban heat island measure technology in the central business district of Osaka city, *Proc. Seventh International Conference on Urban Climate*, 2009